HELDA
HELSINGIN YLIOPISTO
HELSINGFORS UNIVERSITET
UNIVERSITY OF HELSINKI

UNIVERSITY OF HELSINKI

https://helda.helsinki.fi

Chlorophyll fluorescence imaging for monitoring effects of Heterobasidion parviporum small secreted protein induced cell death and in planta defense gene expression.

Wen, Zilan

2019-05-22

Wen , Z , Raffaello , T , Zeng , Z , Pavicic Venegas , M V & Asiegbu , F O 2019 , ' Chlorophyll fluorescence imaging for monitoring effects of Heterobasidion parviporum small secreted protein induced cell death and in planta defense gene expression. ' , Fungal Genetics and Biology , vol. 126 , pp. 37-49 . https://doi.org/10.1016/j.fgb.2019.02.003

http://hdl.handle.net/10138/326973
https://doi.org/10.1016/j.fgb.2019.02.003

cc_by_nc_nd
acceptedVersion

Downloaded from Helda, University of Helsinki institutional repository.

This is an electronic reprint of the original article.

This reprint may differ from the original in pagination and typographic detail.

Please cite the original version.

Chlorophyll fluorescence imaging for monitoring effects of *Heterobasidion parviporum* small secreted protein induced cell death and *in planta* defense gene expression

Authors: Zilan Wen[a], Tommaso Raffaello[a,1], Zhen Zeng[a], Mirko Pavicic[a, b], Fred O. Asiegbu[a,*]

a Faculty of Agriculture and Forestry, P. O. Box 27, Latokartanonkaari 7, 00014, University of Helsinki, Helsinki, Finland

[b] Viikki Plant Science Centre, University of Helsinki, Helsinki, Finland

[1] European Food Safety Authority (EFSA), Via Carlo Magno 1A, 43126 Parma, Italy

* Correspondence: Email: fred.asiegbu@helsinki.fi

ABSTRACT

Heterobasidion parviporum Niemelä & Korhonen is a necrotrophic fungal pathogen of Norway spruce (*Picea abies*). *H. parviporum* genome encodes numerous necrotrophic small secreted proteins (SSP) which might be important for promoting and sustaining the disease development. However, their transcriptional dynamics and plant defense response during infection are largely unknown. In this study, we identified a necrotrophic SSP named HpSSP35.8 and its coding gene was highly expressed in the pre-symptomatic phase of host infection. We explored the impact of HpSSP35.8 on *Nicotiana benthamiana* using *Agrobacterium*-mediated transient expression system under visible spectrum RGB imaging and chlorophyll fluorescence imaging. The results showed that HpSSP35.8 triggered a form of SSP-associated programmed cell death, accompanied by a decrease in the plant photosynthetic activity. Defense-related genes including *WRKY12*, ethylene response factor (*ERF1α*) and a chitinase gene *PR4* were up-regulated in both HpSSP35.8-*N. benthamiana* interaction and *H. parviporum*-Norway spruce pathosystem. It highlighted the potential for the use of chlorophyll fluorescence imaging approach for monitoring indirect effects of SSP as well as for selection of other potential effector-like protein candidates.

Keywords: Necrotrophic pathogen, Norway spruce, Small secreted protein, Defense response, Chlorophyll fluorescence imaging

1. Introduction

Heterobasidion parviporum Niemelä & Korhonen, the causal agent of root and butt rot disease, is the most damaging pathogen of Norway spruce (*Picea abies* (L.) Karst.) in Europe (F.O Asiegbu, Adomas, & Stenlid,

2005). It is a member of the *Heterobasidion annosum* sensu lato complex which consists of four other biological species, including *Heterobasidion annosum* (Fr.) Bref. sensu stricto (s.s.) and *Heterobasidion abietinum* Niemelä & Korhonen in Europe (F.O Asiegbu et al., 2005; Niemelä & Korhonen, 1998), *Heterobasidion irregulare* Garbel. & Otrosina and *Heterobasidion occidentale* Otrosina & Garbel in North America (Otrosina & Garbelotto, 2010). This species complex produces basidiospores mainly contributing to stump primary infection in the field as well as conidiospores commonly applied in spore-infection experiments (Redfern, 1998). Invasive hyphae from infected stump subsequently spread to neighboring uninjured trees through root contacts or grafts (secondary infection) (F.O Asiegbu et al., 2005). The species complex lives as a necrotroph in living tree tissues or as a saprotroph feeding on dead wood (Redfern, 1998), causing tremendous wood decay and economic losses. As a necrotrophic pathogen, it secretes various enzymes (lignin peroxidases, manganese peroxidases, laccase, cytochrome P450 monooxygenases) to disintegrate the plant cell wall and facilitate infection (Yakovlev, Hietala, Steffenrem, Solheim, & Fossdal, 2008).

The secretome analysis of *Heterobasidion* interacting with their host revealed a repertoire of putative small secreted proteins with potential contributions to virulence (Olson et al., 2012; Zeng et al., 2018). However, many *Heterobasidion* SSPs have no predictable domain, no functional description and their roles in pathogenicity remain unknown. Many necrotrophic pathogens (e.g. *Pyrenophora tritici-repentis*) secrete proteinaceous toxins known as effectors that interact with the products of toxin sensitivity genes in the host, leading to disease susceptibility (Deller, Hammond-Kosack, & Rudd, 2011). Some SSPs or effector proteins responsible for disease susceptibility in the host could trigger hypersensitive response (HR)-like cell death reaction in non-host species (Üstün, Müller, Palmisano, Hensel, & Börnke, 2012). The molecular events that lead to HR in plants include accumulation of defense signaling molecules, such as the defense hormones; salicylic acid (SA) or jasmonic acid (JA) and pathogenesis-related proteins (Coll, Epple, & Dangl, 2011). SA generally induces defense against biotrophic pathogens whereas JA and Ethylene (ET) are more likely to activate defense against necrotrophs (Song, Qi, Wasternack, & Xie, 2014; Spoel, Johnson, & Dong, 2007). However, SA- or JA-dependent signaling pathways are not always antagonistic in response to a pathogen. Plants fine tune cross-talk between SA- and JA-dependent defenses by regulatory proteins such as Non-expressor of PR1 (NPR1) (Spoel et al., 2003). Recently, several SSPs from *H. annosum s.l.* were found to be able to cause necrotic cell death response symptoms and induce defense response in non-host plants. A cell

death-inducing protein HaCPL2 from *H. annosum* s.s. induced the expression of both certain SA-responsive genes and JA-responsive genes in *Nicotiana tabacum*, including PR1a, PR2a, PR10 and LOX (Chen, Quintana, Kovalchuk, Ubhayasekera, & Asiegbu, 2015). In addition, Raffaello et.al. (2017) discovered several SSP candidates from *H. irregulare* (HaSSPs) with the ability to induce cell death response in *Nicotiana benthamiana* (Raffaello & Asiegbu, 2017). Especially, HaSSP30 could triggered JA-responsive genes, with induction of PR3, PR4, ERF1a and WRKY12. The above-mentioned study indicates that the defense response in the non-host plant against diverse SSPs in *Heterobasidion* are associated with both SA and JA/ET signaling pathway. Currently, the presence of *H. parviporum* reference genome provides further opportunity to select other potential SSPs. So far very little information is available regarding the transcription of SSPs from *H. parviporum* (HpSSP) on its primary host during pathogen invasion as well as the transcriptional regulation of the signaling genes in host plants during necrotrophic growth.

Chlorophyll fluorescence imaging (CFI) has been utilized to assess plant-pathogen interactions for viruses, bacteria and fungi with biotrophic, hemibiotrophic and necrotrophic life style (Berger, Sinha, & Roitsch, 2007; Chaerle, Hagenbeek, De Bruyne, Valcke, & Van Der Straeten, 2004; Kuckenberg, Tartachnyk, & Noga, 2009; Matouš, Benediktyová, Berger, Roitsch, & Nedbal, 2006; Meyer, Saccardy-Adji, Rizza, & Genty, 2001; Perez-Bueno et al., 2006; Rousseau et al., 2013). CFI is a non-invasive imaging technique based on the fact that light absorbed by chlorophyll molecules in the thylakoid has three possible fates: being used for photosynthesis, dissipated as heat or re-emitted as fluorescence (Murchie & Lawson, 2013). This technique coupled with an automatic high throughput imaging system not only can increase the number of plants analyzed but also improve the time resolution by capturing multiple images at the specific time frame.

In this study, we selected HpSSPs based on their protein sequence similarity to HaSSPs from *H. irregulare*. Transient expression of HpSSPs in *N. benthamiana* was applied to screen putative HpSSPs with *in planta* activity. We hypothesized that HpSSPs inducing necrotic cell death symptoms could be up-regulated in host plants during pathogen invasion. Here we showed that HpSSP35.8 triggered a strong cell death when expressed in *N. benthamiana* leaves *by A. tumefaciens*-mediated infiltration. We analyzed its transcriptional dynamics and explored the effect of HpSSP35.8 on *N. benthamiana* leaves using transient expression system under visible spectrum RGB imaging and CFI. We also focused on the response of defense-related genes against

HpSSP35.8 in *N. benthamiana* as well as defense-related genes against *H. parviporum* colonizing the seedling roots of its host Norway spruce.

2. Materials and methods

2.1. Infection experiment and sample preparation

Norway spruce seeds were kindly provided by Sirkku Pöykkö (Natural Resources Institute Finland, Luke). The spruce seeds were surface sterilized with 30% H_2O_2 for 15 min, rinsed several times with sterilized water and stratified for four days in the dark at 4 °C. The seeds were sown on 1% water agar plates. Half of the plate was overlaid with a piece of moist sterile filter paper before sowing seeds, and then another half piece of filter paper was laid over the seeds. Plates sealed with parafilm were placed in a growth chamber for germination under a photoperiod of 16 h at 20 °C.

Homokaryotic *H. parviporum* isolate 96026 from Åland (courtesy of Kari Korhonen) was maintained on Hagem agar medium (glucose 5 g/L, NH_4NO_3 0.5 g/L, KH_2PO_4 0.5 g/L, $MgSO_4 \cdot 7H_2O$ 0.5 g/L, malt extract 5 g/L, agar 1.5%, and pH = 5) for 3 weeks. Spores were recovered from the surface of mycelia using sterile distilled water. The spore suspension was filtered to remove hyphae remnants, transferred to a new tube, and diluted to a final concentration of 10^6 spores/ml.

Ten Norway spruce germlings (two weeks old) were transferred to a 1% water agar plate with pre-wetted, sterile filter paper. The roots were inoculated with 1 ml of spore suspension, thereafter covered with another piece of moist sterile filter paper. Seedling roots inoculated with 1 ml sterile distilled water served as control. Additional controls included fungal conidiospores and monoculture mycelia pre-grown in Hagem liquid medium. Conidiospore-infected, mock-inoculated root tissues and fungal hyphae were collected over a time course experiment. The roots were immediately frozen in liquid nitrogen and stored at -80 °C until further use. Total RNAs were extracted according to the CTAB method described by Chang et al (Chang, Puryear, & Cairney, 1993).

2.2. Identification and cloning HpSSP-coding genes

The protein sequences of cell death-inducing HaSSPs in *H. irregulare* were utilized to blast against *H. parviporum* secretome by BlastP. The hits in *H. parviporum*, regarded as HpSSPs were used for the functional study. The cloning of HpSSP-coding gene was performed as previously described (Raffaello & Asiegbu, 2017).

HpSSP-coding gene was obtained through gene synthesis (GeneWiz, UK) with codon optimization by removal of internal *BpiI* and *BsaI* restriction sites such that the cleavage sites of these enzymes could be situated on the outside of the fragment. We designed the full-length (+SP) gene to be flanked by BpiI sites (5´-CACCGAAGACACAATG/TAAGCTTCCGTCTTCGTAG-3´) and cloned into the pUC57 plasmid. The gene was transformed into level0 pICH41308 (Addgene, UK) by *BpiI* restriction enzyme (NEB, Finland) and subsequently transferred to level2 pICH86988 (Addgene, UK) by *BsaI* restriction enzyme (NEB, Finland). To generate the genes with C-terminally tagged GFP (with and without signal peptide), the open reading frames were amplified by PCR using the plasmid pICH41308 containing the target sequence. DNA fragment without signal peptide tagged GFP was inserted into the Golden Gate level 0 pICH41308, and full-length DNA fragment tagged GFP was inserted into pAGM1287 (Addgene, UK). Both these two types of the construct were then transferred into the level 2 pICH86988. All cloning steps were done using the Golden Gate cloning approach and *Escherichia coli* TOP10F (Thermo Fisher Scientific, Finland) for selection of positive transformants (Engler, Kandzia, & Marillonnet, 2008; Raffaello & Asiegbu, 2017).

2.3. Transient expression in Nicotiana benthamiana

The transformation of pICH86988-HpSSP vector into *Agrobacterium tumefaciens* GV3101 was performed by the cold shock method as previously described (Raffaello & Asiegbu, 2017). There are three biological replicates for each experiment and *N. benthamiana* plants (two months old) were kept in a growth room under a photoperiod of 16 h at 22 ℃. The leaves collected at 1, 2, and 3 days post inoculation (dpi) were utilized for RNA extraction. Total RNA was extracted using TRI Reagent (Sigma-Aldrich, Finland) based on the manufacturer's instructions.

2.4. Chlorophyll fluorescence imaging

Chlorophyll fluorescence imaging is a non-invasive tool to monitor photosynthetic performance *in vivo*. The chlorophyll fluorescence measurements were performed in plant phenotyping facility at the University of Helsinki Viikki campus (https://www.helsinki.fi/en/infrastructures/national-plant-phenotyping). HpSSP35.8-infiltrated and mock-inoculated tobacco leaves were imaged daily by overhead CCD camera for RGB images positioned in a PlantScreen^{TM} analysis chamber with automated plant transportation between the imaging and watering stations. Chlorophyll fluorescence quenching analysis was performed using FluorCam FC-800MF Pulse Amplitude modulated (PAM, PSI Czech Republic). Plants were dark-adapted for 15 minutes, thereafter

short pulse-modulated light (620 nm) was applied to measure the minimum fluorescence (F_o). A saturating light pulse was applied to determine the maximum fluorescence (F_m). Afterwards, two actinic lights (cool white and red-orange) illuminated the plants for 70 seconds and the chlorophyll fluorescence (F_t) was imaged. Finally, a last saturating light pulse was applied to estimate the maximum fluorescence in light (F'_m). The maximum photochemical efficiency of photosystem II (PSII) is defined as maximum quantum yield (QY max) which was calculated as $(F_m - F_o)/F_m$. The effective efficiency of PSII (ϕ_{PSII}) was determined as $(F'_m – F_t)/ F'_m$. Non-photochemical quenching (NPQ) was determined from $(F_m- F_m')/ F_m'$. RGB images were converted into Hue-Saturation-Brightness (HSB) color space and all three channels were utilized for necrosis analysis.

Using FIJI Is Just ImageJ (FIJI) software (version number: 1.52g), a small circle was drawn on the mock-inoculated area and on HpSSP35.8-infiltrated area for all images and the mean grey value was calculated (Schindelin et al., 2012). Further data analysis and plotting were done using RStudio version 3.4.3 (Team, 2016).

2.5. Quantitative real-time PCR

Primers for qPCR were designed at the Roche Universal Probe Library Assay Design Center (https://lifescience.roche.com/en_fi/brands/universal-probe-library.html#assay-design-center). An equivalent of 1 µg of total RNA was treated with DNase I (Sigma-Aldrich) according to the manufacturer's instructions. Thereafter, complementary DNA (cDNA) was synthesized according to the manufacturer's instruction (Thermo-Fisher Scientific) and the previous study (Raffaello & Asiegbu, 2017). Oligo(dT) primers were used in cDNA synthesis reaction instead of random Hexamers primers. The RNA was reversely transcribed by incubating the reaction mixture for 60 min at 42 °C before pausing the reaction by heating at 70 °C for 5 min. We diluted 3 µl of cDNA in 98 µl of nuclear-free water and pipetted 5.5 µl of diluted cDNA as a template in the qPCR reaction. Apart from the cDNA template, the qPCR reaction mixture consisted of 1 µl of forward primer (10 µm), 1 µl of reverse primer (10 µm) and 7.5 µl of 2X LightCycler 480 SYBR Green I Master (Roche, Finland). The reaction program was as follows: 5 min denaturation at 95 °C, 45 amplification cycles of 10 s at 95 °C, 10 s annealing at 60 °C and extension 20 s at 72 °C.

Normalized relative quantities of HpSSP-coding genes were normalized with four housekeeper genes in *H. parviporum*, including *HpActin*, Cytochrome c oxidase subunit IV (*HpCyt C*), RNA polymerase II transcription factor *(HpRNA Pol2 TF*) and RNA polymerase III transcription factor (*HpRNA Pol3 TF*). Two

HR maker genes (HIN1, Hsr203J) and ten markers for defense-related genes in HpSSP35.8-infiltrated *N. benthamiana* leaves were listed in Table 1 and the qPCR data was normalized by Elongation factor 1 alpha (*NbEF1a*) and *NbActin* with three biological replicates and two technical replicates at each time point. Eight markers for defense-related genes of Norway spruce were *PaPR4*, *PaERF1a*, *PaERF1b*, *PaWRKY12*, *PaLURP1*, *PaPR1*, *PaPAL1*, *PaLOX1*, the gene expressions of which were normalized by *PaEF1a* and *PaUBC1*. Primer specificity was confirmed by melting curve analysis and primer pair efficiency was determined using the standard curve method from serial dilutions of cDNA. Primers for qPCR and their efficiencies were listed in Table 2. The qPCR data were analyzed by the EasyqpcR package in RStudio version 3.4.3 (Hellemans, Mortier, De Paepe, Speleman, & Vandesompele, 2007; Pape, 2017).

3. Results

3.1. HpSSP selection and transient expression in N. benthamiana

The preliminary screening of HpSSPs was based on the protein sequence similarity of HaSSPs in *H. irregulare*. In a previous study, eight SSP candidates showed their ability to cause cell death in *N. benthamiana* (Raffaello & Asiegbu, 2017). BlastP analysis using the eight HaSSPs as queries displayed four hits of hypothetical proteins in *H. parviporum* genome including HpSSP6.141, HpSSP27.89, HpSSP35.8, HpSSP43.64 (summarized in TableS1). We named these hypothetical proteins on the basis of the location of individual coding gene on the corresponding scaffold. To assess the ability of HpSSPs to elicit cell death response that might be associated with effector-like function in plant cells, we transiently expressed the selected SSPs in leaves of *N. benthamiana* by *A. tumefaciens*-mediated infiltration. The results showed no phenotypic alteration for HpSSP6.141 and HpSSP27.89 compared to the control but weak chlorosis for HpSSP43.64. In the case of HpSSP35.8, agro-infiltrated leaves were severely damaged, showing tissue collapse and necrosis at 4 dpi (Fig. 1A).

To investigate the transcriptional dynamics of HpSSP-coding genes in the interaction between *H. parviporum* and Norway spruce germlings, we inoculated spruce roots either with water as mock control or with conidiospores collected from three-week grown mycelia on Hagem solid medium. All samples were collected at 1, 2, 3, 6 and 9 dpi. Three biological replicates were performed at each time point. qPCR revealed that the expression of HpSSP35.8 was highly induced at 2 dpi in infected roots compared with fungal spore.

HpSSP43.64 was significantly expressed at 2 and 3 dpi, while there was no significant induction of HpSSP6.141 and HpSSP27.89 during fungal infection (Fig. 1B). Since HpSSP35.8 was highly induced during pathogen invasion and caused cell death response in *N.benthamiana*, we decided to investigate HpSSP35.8 in more detail.

HpSSP35.8-coding gene has three exons and two introns (Fig. 2A-B), encoding 177 amino acids with a putative signal peptide of 20 amino acids and two cysteine residues (Fig. 2C). HpSSP35.8 shares the same signal peptide and the same site of cysteine residuals with HaSSP30 (Fig. 2C), suggesting that the protein is conserved inter-specifically. A total of 15 homokaryotic isolates of *H. parviporum* that displayed diverse virulence on Norway spruce (Zeng et al., 2018) were also inspected for the presence and divergence of this gene in a previous study. The result showed that two synonymous single nucleotide polymorphisms (SNPs) out of three SNPs were documented in two of these 15 isolates, indicating the gene is highly conserved intra-specifically (Fig. S1).

3.2. In planta expression of HpSSP35.8 during the pre-symptomatic phase of host infection

We performed the infection experiment again with improved time resolution and increasing the bio-replicates from three to five. The normalized relative quantities were monitored from 12 hours over a 9 day post inoculation. The results were compared to control free living mycelia originating from conidiospores at each time point. As previously reported, conidiospores often adhered to the roots, developed germ tubes and hyphae for invasive growth (Li, Osborne, & Asiegbu, 2006). Slight browning on *H. parviporum*-treated roots occurred at 2 dpi. At 3 dpi, much stronger root browning symptom was observed compared to the control treatment (Fig. 3A). The gene was induced as early as 24 hours after spore inoculation, with a peak at 36 hpi (Fig. 3B) coinciding with the formation of the fungal appressoria as previously documented (F.O. Asiegbu, Daniel, & Johansson, 1993). Intriguingly, the expression level decreased considerably at the onset of visible necrosis symptom.

3.3. The effect of HpSSP35.8 on photosynthesis in N. benthamiana by chlorophyll fluorescence imaging

We expressed HpSSP35.8-coding gene in *N. benthamiana* by agroinfiltration to test whether it could trigger a cellular and molecular response in plant cells. The symptom development on leaves was detected simultaneously by RGB and CFI (see the video in the additional file). QY max indicated that the maximum quantum efficiency of photosystem II (PSII) showed a downtrend in the HpSSP35.8-infiltrated but kept steady

in the leaves without HpSSP35.8 (Fig. 4A). QY max difference between treatments was observed at as early as 9 hpi and increased over time together with necrosis progression (Fig. 4A-B). The PSII operating efficiency (ϕ_{PSII}), on the other hand, showed a small decrease in both treatments in the first two hours probably due to the infiltration process. ϕ_{PSII} was more sensitive than QY max in detecting significant differences between the treatments as early as 3 hpi as revealed by a lower value in the leaves infiltrated with HpSSP35.8 than with empty vector (Fig. 4B). NPQ measures the amount of the light energy that is dissipated through non-radiative processes (as heat) to protect against damage by excess light or heat. NPQ had an opposite behaviour to ϕ_{PSII} in early hours. NPQ of both treatments decreased during the first 2 hpi, followed by an apparent difference at 3.75 hpi that the NPQ of HpSSP35.8-infiltrated leaves was higher than that of empty vector-infiltrated leaves. This trend remained until 6 hpi, where both treatments became indistinguishable from each other until almost 13 hpi. At this point NPQ of HpSSP35.8-infiltrated leaves decayed steadily while the control remained stable during the following three days (Fig. 4A-B).

In the Red-Green-Blue (RGB) imaging, the symptoms were not visually evident until 36 hpi (Fig. 4B). To assess the necrosis progression automatically, RGB images were converted into Hue-Saturation-Brightness (HSB) color space and each channel was analyzed separately. Hue is the color or chroma of the pixel in the image, in this case we analyzed how much the color differed from green towards brown. Saturation is how vivid the color is from grey to strong green, while brightness is the level of dark color. In the empty vector infiltrated leaves, these three channels remained relatively unchanged with the exception of brightness that went down and up likely due to leaf movement and change in light reflection (Fig. 4A-B). 'Hue' through the whole analysis remained similar in both treatments until 72 hpi with a small decrease. The infiltration of HpSSP35.8 does not change leaf color but remained green for at around 3 dpi (Fig. 4A-B). 'Saturation' however, showed that HpSSP35.8-infiltrated leaves were not as vivid as the empty vector infiltrated ones, being slightly more sensitive than with visual symptom assessment (Fig. 4A-B). Taken together, these results showed that chlorophyll fluorescence is a very sensitive technique to analyze cell death progression in plants. However, in the absence of fancy equipment, a normal RGB camera can detect differences under the saturation channel.

In order to assess whether the signal peptide contributes to the cell death, we deleted the sequence of the signal peptide and re-cloned it into the level2 vector (pICH86988), we observed that both scenarios could still trigger

the cell death in the leaves (Fig. S2). This suggested that signal peptide does not change the inducing cell-death-activity of the protein. We tried to localize the HpSSP35.8 (+SP): GFP fusion protein and found the GFP-carrying gene also achieved a rapid and strong cell death-related symptom. However, the GFP fluorescence was difficult to visualize.

3.4. HpSSP35.8 triggers defense response during infection of non-host N. benthamiana leaves

In order to investigate the defense signaling molecules underlying the HR-like response, HR gene markers including harpin-induced 1 (*HIN1*) and hypersensitivity-related gene (*Hsr203J*) were studied. HpSSP35.8 induced the expression of HR-related genes. *HIN1* and *Hsr203J* were significantly activated in leaves treated with HpSSP35.8 as compared with the tissue with the empty vector construct. Induction of *HIN1* remained high level at both 1 dpi and 2 dpi while the expression of *Hsr203J* was highest at 1 dpi. Both of them subsequently dropped to control levels at 3 dpi when the tissue was already severely necrotic. This could possibly support the observation that the phenotype alteration might have resulted from SSP-associated cell death.

Besides, we hypothesized that necrotic cell death response would be accompanied by induction of plant immune marker genes. To investigate whether HpSSP35.8 had an effect on the expression of defense-related genes in tobacco leaves, several gene makers involved in JA/ET-dependent signaling pathway (*ERF1a*, *WRKY12*, *PR3, PR4a*), SA-dependent signaling-dependent signaling pathway (*NPR1, PR1a*, *PR2*, *PR5*) and others PR proteins (*Endochitinase*, *protease inhibitor*) were selected for gene expression analysis by qPCR. ERF proteins share a conserved 58-59 amino acids domain binding the GCC box in the promoters of several PR genes (Singh, Foley, & Oñate-Sánchez, 2002). WRKY12 protein has one WRKY domain, a 60 amino acid region containing a conserved sequence of WRKYGQK at its N-terminal together with a zinc-finger-like motif, responsible for binding to DNA sequence (W box) in the target gene promoter region (Eulgem, Rushton, Robatzek, & Somssich, 2000). In our study, both *NbWRKY12* and *NbERF1α* were significantly upregulated at 1 dpi, followed by a decrease of induction during the observation period. This result provided evidence that both *NbERF1α* and *NbWRKY12* contributed to the regulation of defense genes expression in response to the HpSSP35.8 attack in *Nicotiana* leaves. PR proteins produced from plants have anti-microbial activity, such as chitinase that targets fungal cell wall (Kombrink, Sánchez-Vallet, & Thomma, 2011). *NbPR4a*, *NbEndochitinase B* and *NbPI1* genes were remarkably induced at 2 dpi but *NbPR1a*, *NbPR2*, *NbPR3* and

NbPR5 showed no significant difference in HpSSP35.8-infiltrated leaves compared to empty vector treatment. NPR1 (Nonexpressor of pathogenesis-related genes 1), normally regarded as a key regulator of systematic acquired resistance (SAR)-related PR gene expression, was up-regulated in HpSSP35.8-infiltrated tissue (Fig. 5).

3.5. Up-regulation of defense-related genes in Norway spruce seedling roots in response to H. parviporum infection.

We subsequently assessed the activation of defense-related genes in Norway spruce seedling roots after conidiospores inoculation (Fig. 6). The chitinase gene *PaPR4* was rapidly and strongly induced upon pathogen attack. We observed a similar expression pattern in *PaERF1a* and *PaERF1b* which were induced significantly at 60 hpi and remained at a relatively high level compared to control. *PaWRKY12* was upregulated after spore inoculation with a significant induction at 24 hpi. The expression of *PaLURP1* reached its peak at 36 hpi and decreased at 48 hpi at which time the gene was also *in planta* induced significantly during infection with *H. parviporum*. *PaPR1* transcript level was induced from 60 hpi with a peak at 84 hpi before being downregulated. Expression of *PaPAL1* was induced at 96 hpi, while *PaLOX1* was downregulated at 72 hpi.

4. Discussion

HpSSP35.8 is a necrotrophic effector-like protein from a conifer pathogen and is an excellent candidate to investigate the function of necrotrophic small secreted proteins in tree pathosystem. We found four HpSSPs homologs of cell death-inducing HaSSPs, but only HpSSP35.8 has the ability to cause strong cell death in *N. benthamiana*. Consequently, we deduced that not all HpSSP homologs were able to induce cell death in non-host leaves. This may contribute to the fact that *H. parviporum* and *H. irregulare* are two separate species within the *H. annosum* species complex with different host preferences. The study on transcriptional regulation of HpSSPs in its primary host tissues during pathogen invasion suggests that the timing of sample collection is critical in documenting transcriptional changes. The *in planta* expression of the HpSSP35.8-coding gene during host infection also suggested intracellular penetration was achieved as previously documented (F.O. Asiegbu, Daniel, & Johansson, 1994). Transient expression of HpSSP35.8-coding gene by agroinfiltration was able to cause cell death and activate defense response in *N. benthamiana*. We also found that HpSSP35.8 was

highly induced in the early stage of the interaction between the fungus and Norway spruce seedlings, with subsequent induction of host chitinase, WRKY12 and ERF1 transcription factors. These results suggest that HpSSP35.8 probably had a role and relevance in the disease process.

Chlorophyll fluorescence imaging has been utilized for the early detection of fungal infection before symptoms are visible (Bae, Kim, Sicher, Bae, & Bailey, 2006; Prokopová et al., 2010). We focused on three photosynthetic parameters (QY max, ϕ_{PSII} and NPQ) in the *Nicotiana* leaves infiltrated by HpSSP35.8 and empty vector. QY max across many plant species has a robust value of 0.83, which decays quickly in presence of any kind of stress (Björkman & Demmig, 1987). In the Figure 4A, the initial QY max values of both treatments start above 0.8. HpSSP35.8 is likely inducing thylakoid damage and thus a rapid decay in QY max (Havaux & Lannoye, 1983). Besides, HpSSP35.8-infiltrated leaves initially exhibited inhibition of electron transport (φPSII) and increase in non-photochemical chlorophyll fluorescence quenching (NPQ). This is a common plant response in plant-fungal interaction that QY-max and φPSII decline upon infection with an initial rise in NPQ followed by a decline (Rolfe & Scholes, 2010). CFI technique could be a sensitive indicator for screening SSP candidates based on the common photosynthetic response pattern upon SSP infiltration since some of them only induce weakly visible chlorosis. At the late stage, all of these parameters decreased rapidly in HpSSP35.8-infiltrated leaves, inferring that the decay in the plant photosynthetic performance is likely due to thylakoid damage and plant cell death.

The timing of SSP-coding genes expression is crucial as expression normally occurs fast during plant-fungal interaction. HpSSP35.8 displayed a peak induction during the pre-symptomatic phase of host infection, followed by a dramatic reduction after visible necrosis symptoms. This expression pattern has been observed among several plant pathogenic fungi, such as *Stagonospora nodorum* (Liu et al., 2009) and *Zymoseptoria tritici* (Motteram et al., 2009) and could be a common phenomenon. A necrotrophic effector from *S. nodorum* (SnTox3) was highly expressed during hyphal proliferation at the onset of leaf necrosis but decreased considerably once the host tissue became necrotic (Liu et al., 2009). Peak expression of a single NLP effector (MgNLP) from *Z. tritici* was observed during the symptomless phase of colonization of susceptible wheat leaves, followed by a dramatic decrease during disease lesion formation (Motteram et al., 2009). By contrast, a secreted ribonuclease (Zt6) exhibited a double-peak expression pattern during wheat infection, with maximal expression during spore germination immediately following leaf surface inoculation and the second peak

during the necrotrophic phase (Kettles et al., 2018; Rudd et al., 2015). The downregulation of HpSSP35.8 after visible necrosis symptoms on the roots provides some new insight about the potential regulation pattern of this SSP during the life style transition from necrotrophic to saprotrophic life style.

Pathogen recognition in plants are often accompanied by either necrotic cell death or hypersensitive response, a form of programmed cell death localized at the site of pathogen invasion (Coll et al., 2011). Although strong cell death was observed in tobacco leaves in response to HpSSP35.8, the question of whether cell death was triggered by the recognition of HpSSP35.8 or instead of a direct toxic effect of HpSSP35.8 on plant cells is still unknown. We began to address this question by characterizing the expression pattern of HR maker genes in tobacco leaves. The activation of *Hsr203J* and *HIN1* closely links with HR in response to potential effectors or HR-inducing pathogens (Gopalan, Wei, & He, 1996; Pontier, Godiard, Marco, & Roby, 1994; Pontier, Tronchet, Rogowsky, Lam, & Roby, 1998). In this study, both of them were activated preceding the visible appearance of cell death, indicating that the localized cell death in HpSSP35.8-infiltrated leaves could be a form of programmed cell death rather than a direct toxic effect. Upstream of the activation of HR response, the accumulation of diverse plant defense signaling molecules are controlled by signal transduction pathways. Chitinase gene (*NbPR4*) were up-regulated in HpSSP35.8-infiltrated *Nicotiana* leaves. A similar up-regulation of wheat chitinase was observed in the SnTox1-Snn1 interaction, in which the necrotrophic effector SnTox1 binds chitin in the fungal cell wall and protects *Parastagonospora nodorum* from chitinase degradation (Liu et al., 2016; Liu et al., 2012). Not much is known on whether a similar mechanism exists in HpSSP35.8, which merits further study to unravel its mode of action. Moreover, induction of *NbWRKY12* and *NbERF1a* preceding the NbPR4 expression might make sense after transient expression of HpSSP. *WRKY12* in Chinese cabbage (*Brassica rapa*) increased the expression of *BrPR4* and plant defensin *BrPDF1*, markers of the JA signaling pathway (Kim et al., 2014). *ERF1* in *Arabidopsis* is likely to target *Arabidopsis* basic chitinase (*b-CHI*) and *PDF1.2* in response to *B. cinerea* infection (Berrocal-Lobo, Molina, & Solano, 2002; Solano, Stepanova, Chao, & Ecker, 1998). In the case of *N. benthamiana*, the expression of *PR4*, *WRKY12* and *ERF1a* suggested JA/ET-mediated signaling pathway might participate in plant defense against HpSSP35.8 attack. We found that NPR1 in HpSSP35.8-infiltrated leaves was significantly induced, while the robust markers for SA-responsive genes (PR1a, PR2, PR5) were not expressed. *NPR1* is a key regulator of systemic acquired resistance-related PR gene expression (Spoel et al., 2009), translocating to the nucleus and interacting with TGA transcription factors

359 that activate SA-responsive PR genes in *Arabidopsis* (Dong, 2004). However, *NPR1* in *N. attenuate* positively
360 regulated JA-dependent defense during herbivore attack by preventing SA from repressing JA-dependent
361 defenses (Rayapuram & Baldwin, 2007). The role of *NPR1* in the crosstalk between JA- and SA-dependent
362 defense may depend on the plant species and the lifestyle of the pathogen. Here one potential explanation for
363 the expression of *NbNPR1* is that *NPR1* in *N. benthamiana* is involved in JA-/ET-dependent defense against
364 HpSSP35.8.
365 The upregulation of *PR4* together with *ERF1* and *WRKY12* in *H. parviporum*–inoculated spruce suggest that
366 defense-related genes were activated during host infection, but the defense gene accumulation seems to be
367 insufficient as the infected tissue was totally killed by the fungal pathogen. Necrotrophic pathogens often elicit
368 JA and ET-dependent defense to induce a set of PR genes distinct from induced by SA-dependent defense
369 (Spoel et al., 2007). ET/JA-mediated signaling pathways may play a central role in Norway spruce defense
370 response to the necrotrophic *H. parviporum* without antagonism of SA-mediated signaling (Arnerup, Lind,
371 Olson, Stenlid, & Elfstrand, 2011; Arnerup et al., 2013). Here, our data also showed that the SAR marker gene
372 *PR1* in the roots was gradually up-regulated at the initial infection stage, followed by a rapid decrease in
373 comparison to the control. *LURP1*, known as the *PR1* regulon in *Arabidopsis*, was also found to be induced in
374 the seedling roots in this study. The induction of SA-accumulated genes (*PaLURP1* and *PaPR1*) may reveal
375 an accumulation of SA in the early stage of infection, suggesting there is no apparent antagonism between
376 JA/ET and SA pathways (Arnerup et al., 2013). Inoculation with *H. annosum* triggered PAL activity
377 accompanied by an accumulation of free SA in young Norway spruce seedlings. This possibly indicates the
378 exploitation of plant defense by the fungus for promoting infection (Likar & Regvar, 2008). The activation of
379 the SA-mediated signaling pathway could elevate increased susceptibility to the compatible necrotrophic
380 pathogen that is restricted by the JA-dependent plant defense response (Tanaka, Han, & Kahmann, 2015). In
381 our study, the induction of *PR1* and *LURP1* may be an indicator of SA accumulation, which might also have
382 influence in the pathogenicity of *H. parviporum*.

383 **5. Declarations of interest**

384 The authors have no competing interests to declare.

385 **Acknowledgements**

This work was financially supported by Academy of Finland research grant (project no. 276862). We are grateful for support from the Chinese Scholarship Council to Z.W. The funding agencies had no role in study design, data collection and analysis, decision to publish, or preparation of the manuscript.

References

Arnerup, J., Lind, M., Olson, Å., Stenlid, J., & Elfstrand, M. (2011). The pathogenic white-rot fungus *Heterobasidion parviporum* triggers non-specific defence responses in the bark of Norway spruce. *Tree Physiology, 31*(11), 1262-1272. doi:10.1093/treephys/tpr113

Arnerup, J., Nemesio-Gorriz, M., Lundén, K., Asiegbu, F. O., Stenlid, J., & Elfstrand, M. (2013). The primary module in Norway spruce defence signalling against *H. annosum s.l.* seems to be jasmonate-mediated signalling without antagonism of salicylate-mediated signalling. *Planta, 237*(4), 1037-1045. doi:10.1007/s00425-012-1822-8

Asiegbu, F. O., Adomas, A., & Stenlid, J. (2005). Conifer root and butt rot caused by *Heterobasidion annosum* (Fr.) Bref. s.l. *Molecular Plant Pathology, 6*(4), 395-409.

Asiegbu, F. O., Daniel, G., & Johansson, M. (1993). Studies on the Infection of Norway Spruce Roots by *Heterobasidion annosum. Canadian Journal of Botany-Revue Canadienne De Botanique, 71*(12), 1552-1561.

Asiegbu, F. O., Daniel, G., & Johansson, M. (1994). Defense related reactions of seedling roots of Norway spruce to infection by *Heterobasidion annosum* (Fr.) Bref. *Physiological and Molecular Plant Pathology, 45*(1), 1-19. doi:Doi 10.1016/S0885-5765(05)80015-3

Bae, H., Kim, M. S., Sicher, R. C., Bae, H.-J., & Bailey, B. A. (2006). Necrosis- and Ethylene-Inducing Peptide from Fusarium oxysporum Induces a Complex Cascade of Transcripts Associated with Signal Transduction and Cell Death in Arabidopsis. *141*(3), 1056-1067. doi:10.1104/pp.106.076869 %J Plant Physiology

412 Berger, S., Sinha, A. K., & Roitsch, T. (2007). Plant physiology meets phytopathology: plant primary
413 metabolism and plant-pathogen interactions. *Journal of Experimental Botany, 58*(15-16), 4019-4026.
414 doi:10.1093/jxb/erm298
415 Berrocal-Lobo, M., Molina, A., & Solano, R. (2002). Constitutive expression of ETHYLENE-RESPONSE-
416 FACTOR1 in *Arabidopsis* confers resistance to several necrotrophic fungi. *The Plant Journal, 29*(1),
417 23-32. doi:doi:10.1046/j.1365-313x.2002.01191.x
418 Björkman, O., & Demmig, B. (1987). Photon yield of O2 evolution and chlorophyll fluorescence
419 characteristics at 77 K among vascular plants of diverse origins. *Planta, 170*(4), 489-504.
420 doi:10.1007/bf00402983
421 Chaerle, L., Hagenbeek, D., De Bruyne, E., Valcke, R., & Van Der Straeten, D. (2004). Thermal and
422 chlorophyll-fluorescence imaging distinguish plant-pathogen interactions at an early stage. *Plant and*
423 *Cell Physiology, 45*(7), 887-896. doi:DOI 10.1093/pcp/pch097
424 Chen, H. X., Quintana, J., Kovalchuk, A., Ubhayasekera, W., & Asiegbu, F. O. (2015). A cerato-platanin-like
425 protein HaCPL2 from *Heterobasidion annosum sensu stricto* induces cell death in *Nicotiana tabacum*
426 and *Pinus sylvestris*. *Fungal Genetics and Biology, 84*, 41-51. doi:10.1016/j.fgb.2015.09.007
427 Coll, N. S., Epple, P., & Dangl, J. L. (2011). Programmed cell death in the plant immune system. *Cell Death*
428 *and Differentiation, 18*, 1247. doi:10.1038/cdd.2011.37
429 Deller, S., Hammond-Kosack, K. E., & Rudd, J. J. (2011). The complex interactions between host immunity
430 and non-biotrophic fungal pathogens of wheat leaves. *Journal of Plant Physiology, 168*(1), 63-71.
431 doi:https://doi.org/10.1016/j.jplph.2010.05.024
432 Dong, X. (2004). NPR1, all things considered. *Current Opinion in Plant Biology, 7*(5), 547-552.
433 doi:https://doi.org/10.1016/j.pbi.2004.07.005
434 Eulgem, T., Rushton, P. J., Robatzek, S., & Somssich, I. E. (2000). The WRKY superfamily of plant
435 transcription factors. *Trends in Plant Science, 5*(5), 199-206. doi:https://doi.org/10.1016/S1360-
436 1385(00)01600-9
437 Gopalan, S., Wei, W., & He, S. Y. (1996). hrp gene-dependent induction of hin1: a plant gene activated rapidly
438 by both harpins and the avrPto gene-mediated signal. *10*(4), 591-600. doi:doi:10.1046/j.1365-
439 313X.1996.10040591.x

440 Havaux, M., & Lannoye, R. (1983). Chlorophyll fluorescence induction: A sensitive indicator of water stress
441 in maize plants. *Irrigation Science, 4*(2), 147-151. doi:10.1007/bf00273382
442 Kettles, G. J., Carlos, B., A., S. C., Gail, C., Kostya, K., & J., R. J. (2018). Characterization of an antimicrobial
443 and phytotoxic ribonuclease secreted by the fungal wheat pathogen *Zymoseptoria tritici*. *New*
444 *Phytologist, 217*(1), 320-331. doi:doi:10.1111/nph.14786
445 Kim, H. S., Park, Y. H., Nam, H., Lee, Y. M., Song, K., Choi, C., . . . Hwang, D. J. (2014). Overexpression of
446 the *Brassica rapa* transcription factor WRKY12 results in reduced soft rot symptoms caused by
447 *Pectobacterium carotovorum* in *Arabidopsis* and Chinese cabbage. *Plant Biol (Stuttg), 16*(5), 973-981.
448 doi:10.1111/plb.12149
449 Kombrink, A., Sánchez-Vallet, A., & Thomma, B. P. H. J. (2011). The role of chitin detection in plant–
450 pathogen interactions. *Microbes and Infection, 13*(14), 1168-1176.
451 doi:https://doi.org/10.1016/j.micinf.2011.07.010
452 Kuckenberg, J., Tartachnyk, I., & Noga, G. (2009). Temporal and spatial changes of chlorophyll fluorescence
453 as a basis for early and precise detection of leaf rust and powdery mildew infections in wheat leaves.
454 *Precision Agriculture, 10*(1), 34-44. doi:10.1007/s11119-008-9082-0
455 Li, G., Osborne, J., & Asiegbu, F. O. (2006). A macroarray expression analysis of novel cDNAs vital for
456 growth initiation and primary metabolism during development of *Heterobasidion parviporum*
457 conidiospores. *Environmental Microbiology, 8*(8), 1340-1350. doi:10.1111/j.1462-
458 2920.2006.01027.x
459 Likar, M., & Regvar, M. (2008). Early defence reactions in Norway spruce seedlings inoculated with the
460 mycorrhizal fungus *Pisolithus tinctorius* (Persoon) Coker & Couch and the pathogen *Heterobasidion*
461 *annosum* (Fr.) Bref. *Trees, 22*(6), 861-868. doi:10.1007/s00468-008-0247-2
462 Liu, Z., Faris, J. D., Oliver, R. P., Tan, K.-C., Solomon, P. S., McDonald, M. C., . . . Rasmussen, J. B. (2009).
463 SnTox3 acts in effector triggered susceptibility to induce disease on wheat carrying the *Snn3* gene.
464 *Plos Pathogens, 5*(9), e1000581.
465 Liu, Z., Yuanyuan, G., Min, K. Y., D., F. J., L., S. W., M., W. P. J. G., . . . L., F. T. (2016). SnTox1, a
466 Parastagonospora nodorum necrotrophic effector, is a dual-function protein that facilitates infection

while protecting from wheat-produced chitinases. *New Phytologist, 211*(3), 1052-1064. doi:doi:10.1111/nph.13959

Liu, Z., Zhang, Z. C., Faris, J. D., Oliver, R. P., Syme, R., McDonald, M. C., . . . Friesen, T. L. (2012). The cysteine rich necrotrophic effector SnTox1 produced by *Stagonospora nodorum* triggers susceptibility of wheat lines harboring *Snn1*. *Plos Pathogens, 8*(1). doi:ARTN e1002467

10.1371/journal.ppat.1002467

Matouš, K., Benediktyová, Z., Berger, S., Roitsch, T., & Nedbal, L. (2006). Case study of combinatorial imaging: What protocol and what chlorophyll fluorescence image to use when visualizing infection of *Arabidopsis thaliana* by *Pseudomonas syringae*? *Photosynthesis Research, 90*(3), 243-253. doi:10.1007/s11120-006-9120-6

Meyer, S., Saccardy-Adji, K., Rizza, F., & Genty, B. (2001). Inhibition of photosynthesis by *Colletotrichum lindemuthianum* in bean leaves determined by chlorophyll fluorescence imaging. *Plant Cell and Environment, 24*(9), 947-955. doi:DOI 10.1046/j.0016-8025.2001.00737.x

Motteram, J., Kufner, I., Deller, S., Brunner, F., Hammond-Kosack, K. E., Nurnberger, T., & Rudd, J. J. (2009). Molecular characterization and functional analysis of MgNLP, the sole NPP1 domain-containing protein, from the fungal wheat leaf pathogen *Mycosphaerella graminicola*. *Mol Plant Microbe Interact, 22*(7), 790-799. doi:10.1094/MPMI-22-7-0790

Murchie, E. H., & Lawson, T. (2013). Chlorophyll fluorescence analysis: a guide to good practice and understanding some new applications. *Journal of Experimental Botany, 64*(13), 3983-3998. doi:10.1093/jxb/ert208

Niemelä, T., & Korhonen, K. (1998). Taxonomy of the genus Heterobasidion. *Heterobasidion annosum. Biology, ecology, impact and control/Ed. Woodward, S., Stenlid, J., Karjalainen, R. & Hüttermann, A.*

Olson, Å., Aerts, A., Asiegbu, F., Belbahri, L., Bouzid, O., Broberg, A., . . . Dalman, K. (2012). Insight into trade-off between wood decay and parasitism from the genome of a fungal forest pathogen. *New Phytologist, 194*(4), 1001-1013.

Otrosina, W. J., & Garbelotto, M. (2010). *Heterobasidion occidentale* sp. nov. and *Heterobasidion irregulare* nom. nov.: a disposition of North American *Heterobasidion* biological species. *Fungal Biology, 114*(1), 16-25.

Perez-Bueno, M. L., Ciscato, M., vandeVen, M., Garcia-Luque, I., Valcke, R., & Baron, M. (2006). Imaging viral infection: studies on *Nicotiana benthamiana* plants infected with the pepper mild mottle tobamovirus. *Photosynthesis Research, 90*(2), 111-123. doi:10.1007/s11120-006-9098-0

Pontier, D., Godiard, L., Marco, Y., & Roby, D. (1994). hsr203J, a tobacco gene whose activation is rapid, highly localized and specific for incompatible plant/pathogen interactions. *5*(4), 507-521. doi:doi:10.1046/j.1365-313X.1994.05040507.x

Pontier, D., Tronchet, M., Rogowsky, P., Lam, E., & Roby, D. (1998). Activation of hsr203, a Plant Gene Expressed During Incompatible Plant-Pathogen Interactions, Is Correlated with Programmed Cell Death. *Molecular Plant-Microbe Interactions, 11*(6), 544-554. doi:10.1094/MPMI.1998.11.6.544

Prokopová, J., Špundová, M., Sedlářová, M., Husičková, A., Novotný, R., Doležal, K., . . . Lebeda, A. (2010). Photosynthetic responses of lettuce to downy mildew infection and cytokinin treatment. *Plant Physiology and Biochemistry, 48*(8), 716-723. doi:https://doi.org/10.1016/j.plaphy.2010.04.003

Raffaello, T., & Asiegbu, F. O. (2017). Small secreted proteins from the necrotrophic conifer pathogen *Heterobasidion annosum s.l.* (HaSSPs) induce cell death in *Nicotiana benthamiana*. *Scientific Reports, 7*(1), 8000. doi:10.1038/s41598-017-08010-0

Rayapuram, C., & Baldwin, I. T. (2007). Increased SA in NPR1-silenced plants antagonizes JA and JA-dependent direct and indirect defenses in herbivore-attacked Nicotiana attenuata in nature. *The Plant Journal, 52*(4), 700-715. doi:10.1111/j.1365-313X.2007.03267.x

Redfern, D. B. (1998). Spore dispersal and infection. *Heterobasidion annosum. Ecology, impact and control*, 105-124.

Rolfe, S. A., & Scholes, J. D. (2010). Chlorophyll fluorescence imaging of plant–pathogen interactions. *Protoplasma, 247*(3), 163-175. doi:10.1007/s00709-010-0203-z

Rousseau, C., Belin, E., Bove, E., Rousseau, D., Fabre, F., Berruyer, R., . . . Boureau, T. (2013). High throughput quantitative phenotyping of plant resistance using chlorophyll fluorescence image analysis. *Plant methods, 9*. doi:Artn 17

10.1186/1746-4811-9-17

Rudd, J., Kanyuka, K., Hassani-Pak, K., Derbyshire, M., andongabo, a., Devonshire, J., . . . Courbot, M. (2015). Transcriptome and metabolite profiling the infection cycle of *Zymoseptoria tritici* on wheat reveals a

biphasic interaction with plant immunity involving differential pathogen chromosomal contributions, and a variation on the hemibiotrophic lifestyle definition. *Plant Physiology*. doi:10.1104/pp.114.255927

Singh, K. B., Foley, R. C., & Oñate-Sánchez, L. (2002). Transcription factors in plant defense and stress responses. *Current Opinion in Plant Biology, 5*(5), 430-436. doi:https://doi.org/10.1016/S1369-5266(02)00289-3

Solano, R., Stepanova, A., Chao, Q., & Ecker, J. R. (1998). Nuclear events in ethylene signaling: a transcriptional cascade mediated by ETHYLENE-INSENSITIVE3 and ETHYLENE-RESPONSE-FACTOR1. *Genes Dev, 12*(23), 3703-3714.

Song, S., Qi, T., Wasternack, C., & Xie, D. (2014). Jasmonate signaling and crosstalk with gibberellin and ethylene. *Current Opinion in Plant Biology, 21*, 112-119. doi:https://doi.org/10.1016/j.pbi.2014.07.005

Spoel, S. H., Johnson, J. S., & Dong, X. (2007). Regulation of tradeoffs between plant defenses against pathogens with different lifestyles. *104*(47), 18842-18847. doi:10.1073/pnas.0708139104 %J Proceedings of the National Academy of Sciences

Spoel, S. H., Koornneef, A., Claessens, S. M. C., Korzelius, J. P., Van Pelt, J. A., Mueller, M. J., . . . Pieterse, C. M. J. (2003). NPR1 Modulates Cross-Talk between Salicylate- and Jasmonate-Dependent Defense Pathways through a Novel Function in the Cytosol. *15*(3), 760-770. doi:10.1105/tpc.009159 %J The Plant Cell

Spoel, S. H., Mou, Z., Tada, Y., Spivey, N. W., Genschik, P., & Dong, X. (2009). Proteasome-Mediated Turnover of the Transcription Coactivator NPR1 Plays Dual Roles in Regulating Plant Immunity. *Cell, 137*(5), 860-872. doi:https://doi.org/10.1016/j.cell.2009.03.038

Tanaka, S., Han, X. W., & Kahmann, R. (2015). Microbial effectors target multiple steps in the salicylic acid production and signaling pathway. *Frontiers in Plant Science, 6*. doi:10.3389/fpls.2015.00349

Üstün, Ş., Müller, P., Palmisano, R., Hensel, M., & Börnke, F. (2012). SseF, a type III effector protein from the mammalian pathogen Salmonella enterica, requires resistance-gene-mediated signalling to activate cell death in the model plant Nicotiana benthamiana. *194*(4), 1046-1060. doi:doi:10.1111/j.1469-8137.2012.04124.x

551 Yakovlev, I. A., Hietala, A. M., Steffenrem, A., Solheim, H., & Fossdal, C. G. (2008). Identification and
552 analysis of differentially expressed *Heterobasidion parviporum* genes during natural colonization of
553 Norway spruce stems. *Fungal Genetics and Biology, 45*(4), 498-513. doi:10.1016/j.fgb.2007.10.011
554 Zeng, Z., Sun, H., Vainio, E. J., Raffaello, T., Kovalchuk, A., Morin, E., . . . Asiegbu, F. O. (2018). Intraspecific
555 comparative genomics of isolates of the Norway spruce pathogen (*Heterobasidion parviporum*) and
556 identification of its potential virulence factors. *Bmc Genomics, 19*(1), 220. doi:10.1186/s12864-018-
557 4610-4

558

559

560 **Figure and table legends**

561 Fig. S1 Nucleotides alignment of HpSSP35.8 over 15 *H.parviporum* isolates. The columns highlighted in grey
562 are the sites of synonymous single nucleotide polymorphisms (SNPs) and in yellow is the site of non-
563 synonymous SNPs. The changed nucleotides are marked in red. S1-S15 are the names of *H. parviporum*
564 isolates previously collected across Finland.

565 Fig. S2 Cell death was induced by full-length *HpSSP35.8* (+SP), full-length *HpSSP35.8* containing green
566 fluorescent protein (+GFP) as well as *HpSSP35.8* without signal peptide (-SP) during 2-6 days post infiltration.
567 Asterisk indicates the infiltration site.

568 Supplementary file (Video): The progress of necrosis in HpSSP35.8-infiltrated leaves under RGB imaging
569 and chlorophyll fluorescence imaging. The side labelled A of leaves was inoculated with *A. tumefaciens*
570 containing an empty vector as the control. The side B of leaves was infiltrated with *A. tumefaciens* containing
571 pICH86988 with HpSSP35.8 insert as the treatment.

572 Table 1 Summary of primer sets used in *N. benthamiana* and in *H. parviporum.*

573 Table 2 Summary of primer sets for defense-related genes in *Picea abies*.

574 Table S1 Four HpSSP homologs in *H. parviporum* of HaSSPs.

575 Fig. 1 Transient expression of HpSSPs in *N. benthamiana* and HpSSPs expression in spruce seeding. (A)
576 Putative HpSSP selection based on activation of necrosis cell death response in agroinfiltrated-*N. benthamiana*
577 leaves. Agroinfiltration was performed on the right side of a leaf with pICH86988 vector carrying HpSSP
578 individuals and the left side of the same leaf with empty vector as control. (B) Expression dynamics of HpSSPs

in conidiospore-inoculated seedling roots. Normalized relative quantification of HpSSPs was scaled relative to fungal conidiospores. Four reference genes used in the study are *HpActin, HpCyt C, HpRNA Pol2 TF, HpRNA Pol3 TF*. Error bars represent the SD from three independent experiments. Asterisks indicate significant difference as assessed by Student's t-test ($p < 0.001$: ***; $p < 0.01$: **; $p < 0.05$: *).

Fig. 2 Gene structure, nucleotide and amino acid sequences of HpSSP35.8. (A) Gene structure of HpSSP35.8-coding gene. (B) Nucleotide sequence of HpSSP35.8. The nucleotide sequences highlighted in green indicate the intron. The fragments highlighted in yellow indicate the *BsaI* and *BpiI* restriction sites. The orange sequences indicate the primer sites used to amplify the genomic region for qPCR. (C) Amino acid sequence alignment of HpSSP35.8 with its homologue HaSSP30 from *H. irregulare*. The bold amino acids indicate the predicted signal peptides. The cysteine residues are in yellow.

Fig. 3 Expression dynamics of HpSSP35.8 in conidiospore-inoculated seedling roots. (A) The browning symptom appeared at 2-3 dpi. Spore inoculum was used as treatment and distilled water was used as the control. (B) Gene expression of HpSSP35.8 in infected roots. Normalized relative qualification of HpSSP35.8 was scaled to pure mycelia cultured in malt extract liquid medium. Four reference genes used in the study are *HpActin, HpCyt C, HpRNA Pol2 TF, HpRNA Pol3 TF*. Error bars represent the SD from five independent experiments. Asterisks indicate significant difference as assessed by Student's t-test ($p < 0.001$: ***; $p < 0.01$: **; $p < 0.05$: *).

Fig. 4 Necrosis progression in agroinfiltrated-*N. benthamiana* leaves detected by using Red-Geen-Blue (RGB) imaging and chlorophyll fluorescence imaging (CFI). (A) Photochemical reactions on leaves including maximum quantum efficiency of photosystem II (QY max), PSII operating efficiency (ϕ_{PSII}), Non-Photochemical Quenching (NPQ) within 96 hours. RGB imaging was converted into Hue-Saturation-Brightness color space. (B) The cell death development under RGB image and QY-max image at 3, 12, 36, 72 hours post-infiltration (hpi). Agroinfiltration was performed on one side of a leaf with pICH86988 vector carrying full-length of HpSSP35.8 containing signal peptide (+SP) and another side of the same leaf with empty vector as control (C).

Fig. 5 Expression analysis of defense-related genes in HpSSP35.8-infiltrated leaves of *N. benthamiana*. Normalized qualification of defense-related genes of *HpSSP35.8*-infiltrated leaves (HpSSP35.8) is shown relative to empty vector-infiltrated leaves (Empty vector). Reference genes were *NbEF1a* and *NbActin*. Genes

chosen for analysis were as follows: (A) Harpin-induced 1 (*NbHIN1*); (B) Hypersensitivity-related gene (*NbHsr203J*); (C) Ethylene response factor-1a (*NbERF1a*); (D) WRKY DNA-binding protein 12 (*NbWRKY12*); (E) Pathogenesis-related gene 4a (*NbPR4a*); (F) Endochitinase B in *N. benthamiana* (*NbEndochitinase B*); (G) Proteinase inhibitor 1; (H) Nonexpressor Of PR1 (*NbNPR1*); (I) Pathogensis-related gene 1 a (*NbPR1a*); (J) Pathogensis-related gene 2 (*NbPR2*); (K) Pathogenesis-related gene 3 (*NbPR3*); (L) Pathogenesis-related gene 5 (*NbPR5*). Error bars represent the standard deviation (SD) from three independent experiments. Asterisks indicate significant difference from empty vector-infiltrated leaves as assessed by Student's *t*-test ($p < 0.001$: ***; $p < 0.01$: **; $p < 0.05$: *).

Fig. 6 Expression analysis of selected differentially regulated defense-related genes in Norway spruce seedling roots in response to *H. parviporum*. Normalized qualification of defense-related genes of infected roots (treatment) is shown relative to water-treated roots (control). Reference genes are *PaFE1a,* and *PaUBC1*. Genes chosen for analysis were as follows: (A) Chitinase gene PR4a (*PaPR4a*); (B) Ethylene response factor-1a (*PaERF1a*); (C) Ethylene response factor-1b (*PaERF1b*); (D) WRKY DNA-binding protein 12 (*PaWRKY12*); (E) Late up-regulated in response to *Hyaloperonospora parasitica* (*PaLURP1*); (F) Pathogensis-related gene 1 (*PaPR1*); (G) Phenylalanine ammonia-lyase (*PaPAL1*); (H) Lipoxygenase (*PaLOX1*). Error bars represent the SD from three independent experiments. Asterisks indicate significant difference from water-inoculated roots as assessed by Student's *t*-test ($p < 0.001$: ***; $p < 0.01$: **; $p < 0.05$: *).

625 **Table 1** Summary of primer sets used in *N. benthamiana* and in *H. parviporum*

Primer		(5'-3')	Product size (nt)	Efficiency	Gene annotation	Reference
NbActin	Forward	TACCACCGGTATTGTGTTGG	60	1.82	Actin	Tommaso, 2017
	Reverse	TCATAAATTGGGACGGTGTG				
NbEF1a	Forward	CTCCTTGAGGCTCTTGACCA	60	1.91	Eongation factor alpha	Tommaso, 2017
	Reverse	ACGTAGGGGTTTGTCTGTGG				
NbHIN1	Forward	TCAGTTCGATTTGTCCACCA	NA	1.82	Harpin-induced 1	(Üstün, Müller, Palmisano, Hensel, & Börnke, 2012)
	Reverse	TGAATACTGGACGCAAGCTG				
NbHsr203J	Forward	GGCTCAACGATTACGCAGAT	NA	1.872	Hypersensitivity-related gene	(Üstün, Müller, Palmisano, Hensel, & Börnke, 2012)
	Reverse	CGGGGTTTGCTCTTGTTCTA				
NbERF1a	Forward	GTTAACGCCGTCAAGTTGGT	72	1.93	Ethylene response factor	Tommaso, 2017
	Reverse	AGAGGCGGCACCTCAAATA				
NbWRKY12	Forward	CTCATCAGCTAGTTCATTTGATGC	NA	2	WRKY family transcription factor	Tommaso, 2017
	Reverse	AGCTCGGTCTTTGTTCTAAAAGC				
NbPR4a	Forward	CAACCCACAGAACATTAACTGG	69	1.9	Pathogenesis-related gene 4	Tommaso, 2017
	Reverse	TTGTCGGCATCCCAAGTAGT				
NbEndochitinase. B	Forward	GCCTTTATCAATGCTGCTAGG	67	1.88	Chitinase activity, chitin binding	Tommaso, 2017
	Reverse	ATCCTCGGGCAGTAGTATCG				
NbPI1	Forward	CTTCAAAGACTATGGTGAAGTTTGC	NA	2	Protease inhibitor	Tommaso, 2017
	Reverse	CAGACTGAGACACATCAAGTTGC				
NbNPR1	Forward	AGGACCGGTTATGCATTGAG	64	1.816	Nonexpressor of PR genes1	In this study
	Reverse	GCTTCTCCTAGCAGTGGATCTC				
NbPR5	Forward	ATGCGCAGCCCCTATTAAC	67	1.88	Pathogenesis-related gene 5, Thaumatin-like protein	Tommaso, 2017
	Reverse	TGGGTTGTTACATCCACCTTG				
NbPR1a	Forward	CGACCAGGTAGCAGCCTATG	NA	2	Pathogenesis-related gene 1	Tommaso, 2017
	Reverse	TCTCAACAGCCTTAGCAGCC				
NbPR2	Forward	GGGCTGTTAATTTGCAGTATCC	NA	2	Pathogenesis-related gene 2	Tommaso, 2017
	Reverse	GGTTTATAACATCTTGGTCTGATGG				
NbPR3	Forward	TGCCTTTTTCGGTCAAACTT	64	1.87	Pathogenesis-related gene 3	Tommaso, 2017
	Reverse	TGTAAATGGTTCTGCACTCAGG				
HpActin	Forward	ACCCAGCATCGAGATCCAAG	192	1.721	Actin	Tommaso, 2013

	Reverse	GTCACTCTTGCAGTCAACAC				
HpCyt C	Forward	ATTCCGCTGTCGAACGTC	109	1.812	Cytochrome c oxidase subunit IV	Tommaso, 2013
	Reverse	TGAGCTCCTTCCAGTCCTTC				
HpRNA Pol2 TF	Forward	GGGTTCGATTGTCAGGATGT	76	1.975	RNA polymerase II transcription factor	Tommaso, 2013
	Reverse	CAGCAATGTCAGACACAAACTT				
HpRNA Pol3 TF	Forward	AACAAGATGCGCTGGAAAG	94	2.017	RNA polymerase III transcription factor	Tommaso, 2013
	Reverse	GGAGCTCCTCACAATTTGGT				
HpSSP6.141	Forward	CGTCCCTCTCGCTGCTATTT	141	1.721	Hypothetical protein	In this study
	Reverse	ATTGACGGCACCATCACAGT				
HpSSP27.89	Forward	GCGGAGATCATGCTGAGGAA	105	2.05	Hypothetical protein	In this study
	Reverse	CTTCTCCAACAGCAGAGCCA				
HpSSP35.8	Forward	CCGCGCAGAACAAGAAGATC	168	2.023	Hypothetical protein	In this study
	Reverse	TGCTGGTGTGGAAGTCGTTT				
HpSSP43.64	Forward	GATGCTTCAAGTTCGTCGGC	140	1.949	Hypothetical protein	In this study
	Reverse	GTAGTGGAAGCGGCAGAAGA				

Table 2 Summary of primer sets for defense-related genes in *Picea abies*

Primer name		5'-3'	Product size (nt)	Efficiency	Gene prediction	Arabidopsis homolog locus	*Picea abies*
PaEF1α	Forward	TGTGGAAGTTTGAGACAAACAAA	121	1.859	elongation factor alpha	NA	MA_434977g0010
	Reverse	TCAATGATCAAAACTGCACAATC					
PaUBC1	Forward	GTCCTGCATTGACCATCTCTAA	113	1.945	Ubiquitin-conjugating enzyme	AT1G64230	MA_10437205g0010
	Reverse	CCTGTCAGTTTTGTACATGTGAGC					
PaPR4	Forward	GCATAACTGGGATCTCAATGC	93	2.001	pathogenesis-related gene 4, response to ethylene	AT3G04720	MA_321399g0010
	Reverse	GCCGTCCAACCGTATTTCT					
PaERF1a	Forward	CGAAGACTGTGAAGAACAATGC	94	1.974	ethylene response factor	AT4G17500	MA_166248g0010
	Reverse	CGCGAAGAGTCCCTTATCTC					
PaERF1b	Forward	CGCCAAGAAGGGATGGAT	62	1.984	ethylene response factor	AT3G23240	MA_5805979g0010
	Reverse	CGGCTTCCTTCTTCGTCTC					
PaWRKY12	Forward	AGGTCGTTAAAAGTAGCCCTCA	67	2.025	WRKY family transcription factor	AT2G44745	MA_23415g0010
	Reverse	TTCACGCTGCAATTGTTTTC					
PaLURP1	Forward	AAACGAATTCTGAGAGACCAACA	72	2.043	Late up-regulated in response to *Hyaloperonospora parasitica*	AT2G14560	MA_44963g0010
	Reverse	CTCGTGAAGGCTCAGCAACT					
PaPR1	Forward	ATGCACGCAATTATGCAAGA	63	1.896	molecular marker for the SAR response	AT2G14610	MA_10392069g0010
	Reverse	AGGGGCTGTCCGAGTGTT					
PaPAL1	Forward	GGATTCTGGAGGCCATGA	80	2.094	Phenylalanine ammonia lyase	AT2G37040	MA_10429279g0010
	Reverse	GGACGCCGTTATCGTACCT					
PaLOX1	Forward	ACGGGCTAACAGTTGAGCAG	64	2.162	Lipoxygenase	AT1G55020	MA_47100g0010
	Reverse	ACGTCATGGTGGTCCAGAA					

635

636

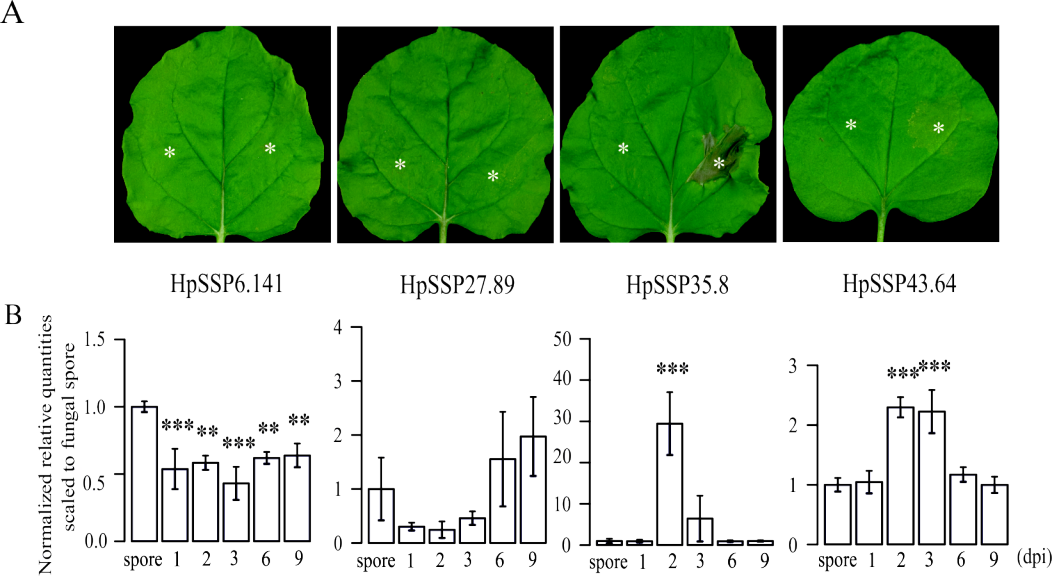
A
HpSSP6.141
HpSSP27.89
HpSSP35.8
HpSSP43.64
B
Normalized relative quantities scaled to fungal spore
spore 1 2 3 6 9 (dpi)

A

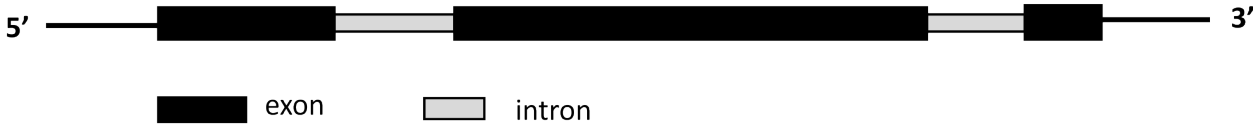

B

>evm.scaffold35.8_genomics_gene

atgcaattcaaatacctcatcgctctttctgctctcctgctctcgagcacggtcattgcggccccttacctgag[gttcgtgcacacttactcctgtt
gatgttgccatctgctgaacctgacatccctggtag]ggcacaaccaacgacgtcgttctccaacgccgatcggtctcccctcatacacgttcac
caacgacttggccgacatcgtgatccccgcccccctccccgcgaccgctgctaagaaagccatcgccgcgcagaacaagaagatcacaaagg
caaaggcgaaccaaaaggcgaaggaagccctccagaagaccgcgtcgtcgcacgtcaccaccgtccttaacgcggccgctggcaccctgaa
cctcagcgggaaccttgcggtcaaggtcacaaacgacttccacaccagcaaggacccggagagccacgcgacgttcgagttctctgcgactgc
ttgtggcgggacgtgcgtcggccatgcgtacaagtcgccctcgaaaatctcgccgggcaagggccagcccggcaaaatcttcagcgccgggca
tgctgttattttcggg[gtaagtccgtcccgtcccgcatgcactcttttaattgctcataatatctgttggaaacag]ggcagcgataaatga*

C

```
HpSSP35.8       MQFKYLIALSALLLSSTVIAAPLPEGTTNDVVLQRRSVSPSYTFTNDLAD
HaSSP30         MQFKYLIALSALLLSSTVIAAPLPEGTTNDVI LQRRSVSPSFTFTNDLAN
                ******************************* :********* :********:

HpSSP35.8       IVIPAPPPATAAKKAIAAQNKKITKAKANQKAKEALQKTASSHVTTVLNA
HaSSP30         IVIPAPLPATAAKKAIAAQEKKIKKAQANQKAKEALQKTASSHVTTVLNA
                ****** ************ :***. ** :  ************************

HpSSP35.8       AAGTLNLSGNLAVKVTNDFHTSKDPESHATFEFSATACGGTCVGHAYKSP
HaSSP30         AADTLKLSGSLAVKVTNDFHTSKDPESHATFEFSAPACGGTCVGHAYKSP
                **. **:  ***.*****************************.***************

HpSSP35.8       SKISPGKGQPGKIFSAGHAVIFGGSDK
HaSSP30         SKISPGKGQPGKIFSAGHAVIFGGSDK
                ****************************
```

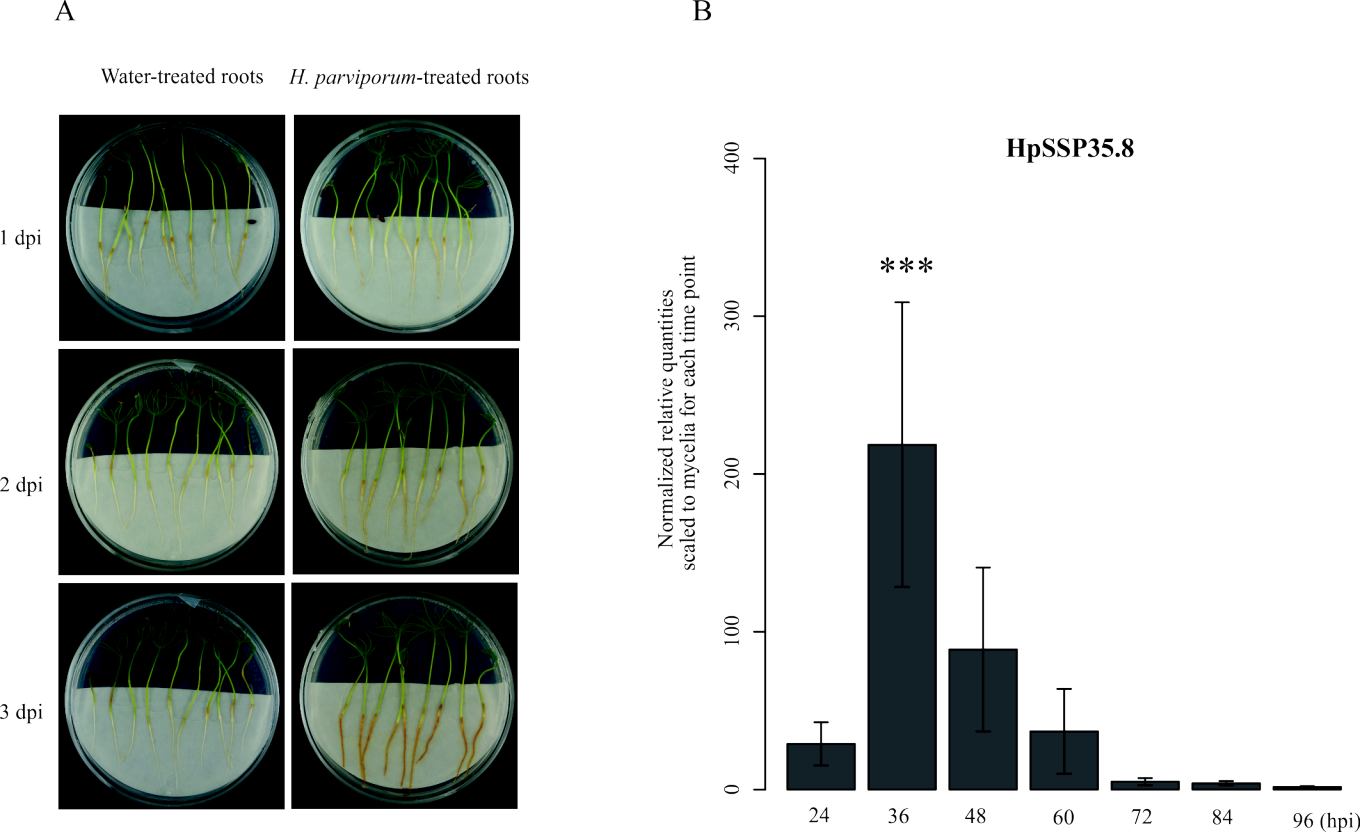
A
Water-treated roots
H. parviporum-treated roots
1 dpi
2 dpi
3 dpi
B
HpSSP35.8
Normalized relative quantities
scaled to mycelia for each time point
***
0
100
200
300
400
24
36
48
60
72
84
96 (hpi)

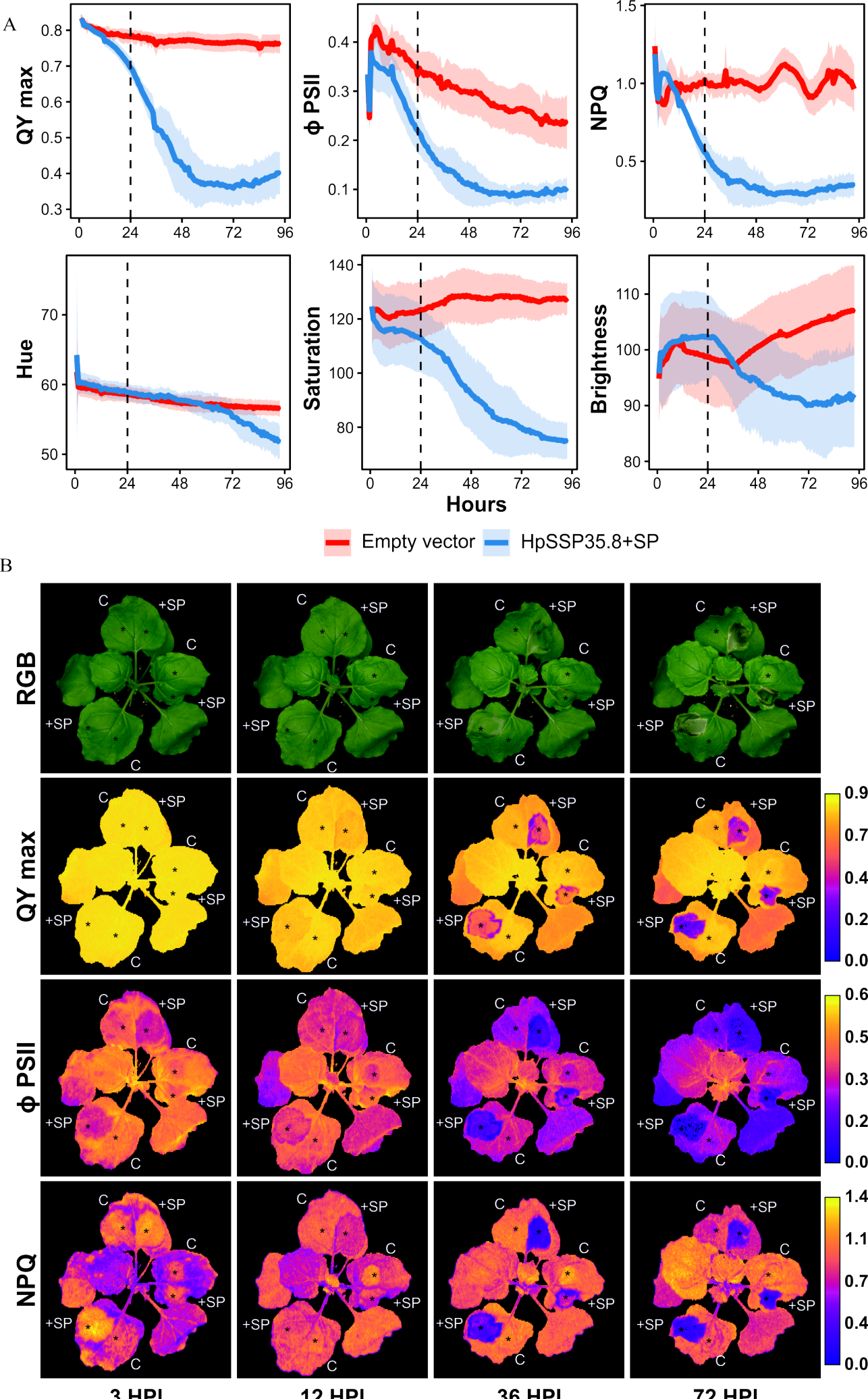
A
QY max
ϕ PSII
NPQ
Hue
Saturation
Brightness
Hours
Empty vector
HpSSP35.8+SP
B
RGB
QY max
ϕ PSII
NPQ
C
+SP
3 HPI
12 HPI
36 HPI
72 HPI

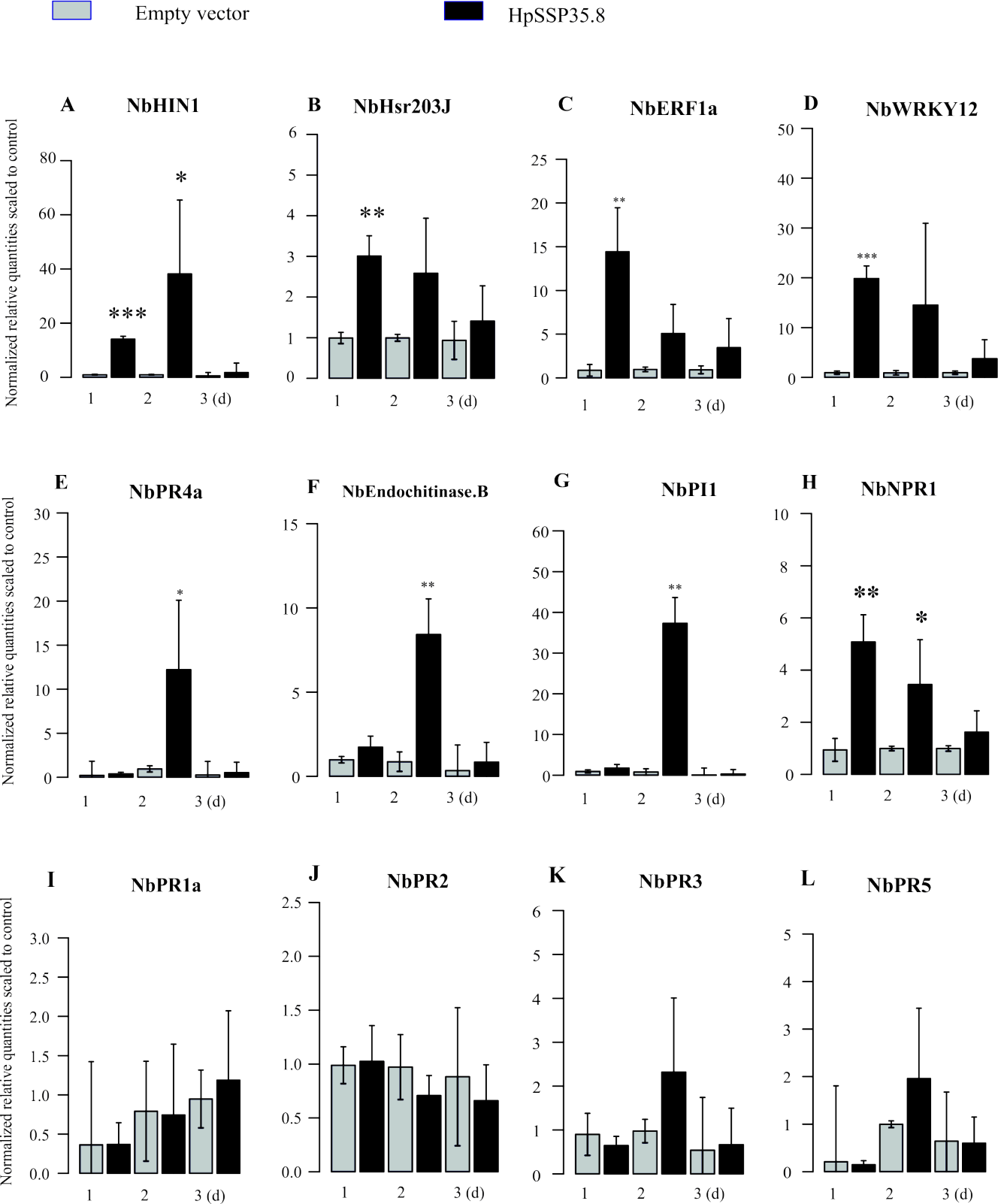
Empty vector
HpSSP35.8
A
NbHIN1
B
NbHsr203J
C
NbERF1a
D
NbWRKY12
E
NbPR4a
F
NbEndochitinase.B
G
NbPI1
H
NbNPR1
I
NbPR1a
J
NbPR2
K
NbPR3
L
NbPR5
Normalized relative quantities scaled to control
1
2
3 (d)

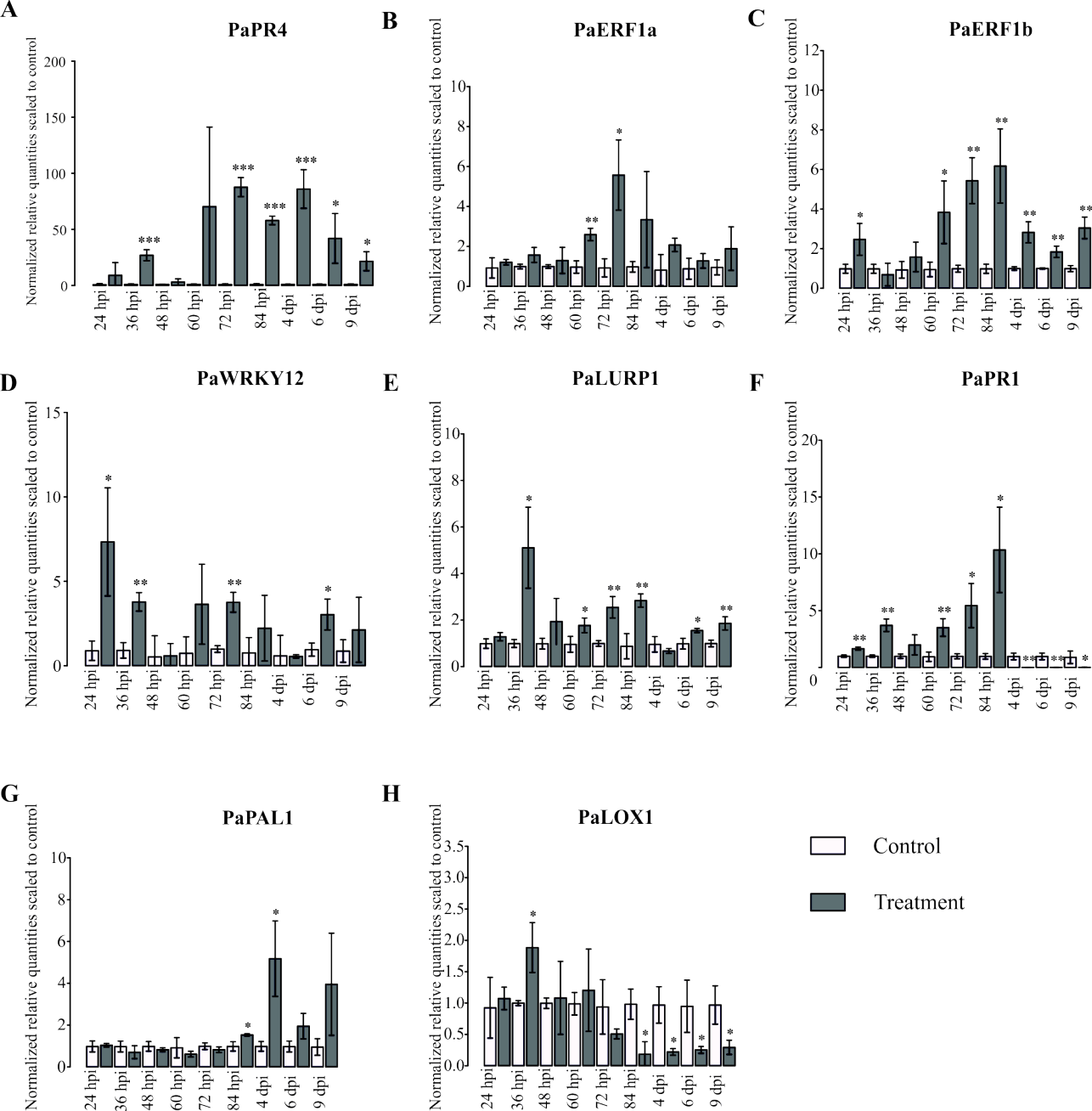
A
PaPR4
B
PaERF1a
C
PaERF1b
D
PaWRKY12
E
PaLURP1
F
PaPR1
G
PaPAL1
H
PaLOX1
Normalized relative quantities scaled to control
24 hpi
36 hpi
48 hpi
60 hpi
72 hpi
84 hpi
4 dpi
6 dpi
9 dpi
Control
Treatment

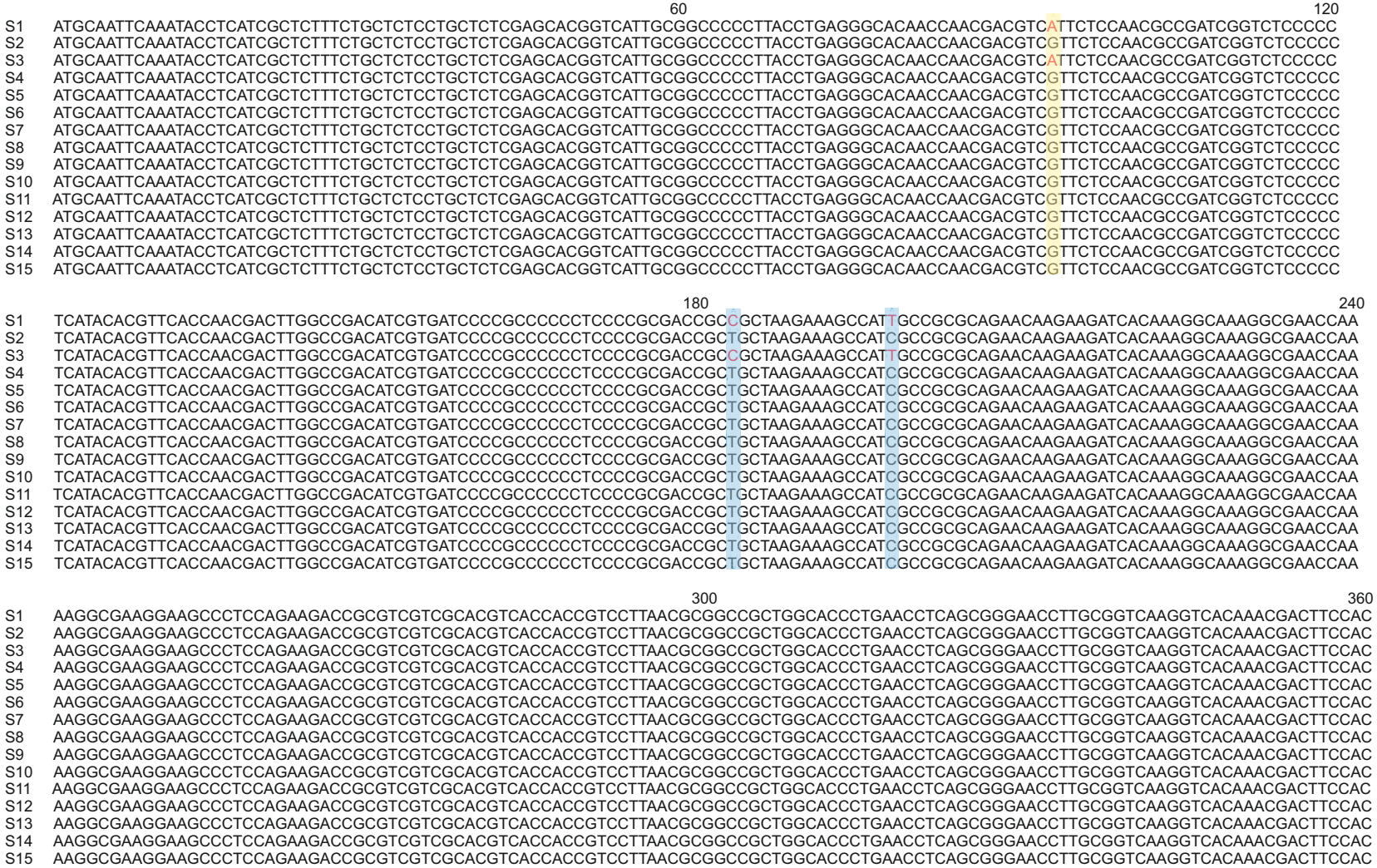
60
120
S1 ATGCAATTCAAATACCTCATCGCTCTTTCTGCTCTCCTGCTCTCGAGCACGGTCATTGCGGCCCCCTTACCTGAGGGCACAACCAACGACGTCATTCTCCAACGCCGATCGGTCTCCCCC
S2 ATGCAATTCAAATACCTCATCGCTCTTTCTGCTCTCCTGCTCTCGAGCACGGTCATTGCGGCCCCCTTACCTGAGGGCACAACCAACGACGTCGTTCTCCAACGCCGATCGGTCTCCCCC
S3 ATGCAATTCAAATACCTCATCGCTCTTTCTGCTCTCCTGCTCTCGAGCACGGTCATTGCGGCCCCCTTACCTGAGGGCACAACCAACGACGTCATTCTCCAACGCCGATCGGTCTCCCCC
S4 ATGCAATTCAAATACCTCATCGCTCTTTCTGCTCTCCTGCTCTCGAGCACGGTCATTGCGGCCCCCTTACCTGAGGGCACAACCAACGACGTCGTTCTCCAACGCCGATCGGTCTCCCCC
S5 ATGCAATTCAAATACCTCATCGCTCTTTCTGCTCTCCTGCTCTCGAGCACGGTCATTGCGGCCCCCTTACCTGAGGGCACAACCAACGACGTCGTTCTCCAACGCCGATCGGTCTCCCCC
S6 ATGCAATTCAAATACCTCATCGCTCTTTCTGCTCTCCTGCTCTCGAGCACGGTCATTGCGGCCCCCTTACCTGAGGGCACAACCAACGACGTCGTTCTCCAACGCCGATCGGTCTCCCCC
S7 ATGCAATTCAAATACCTCATCGCTCTTTCTGCTCTCCTGCTCTCGAGCACGGTCATTGCGGCCCCCTTACCTGAGGGCACAACCAACGACGTCGTTCTCCAACGCCGATCGGTCTCCCCC
S8 ATGCAATTCAAATACCTCATCGCTCTTTCTGCTCTCCTGCTCTCGAGCACGGTCATTGCGGCCCCCTTACCTGAGGGCACAACCAACGACGTCGTTCTCCAACGCCGATCGGTCTCCCCC
S9 ATGCAATTCAAATACCTCATCGCTCTTTCTGCTCTCCTGCTCTCGAGCACGGTCATTGCGGCCCCCTTACCTGAGGGCACAACCAACGACGTCGTTCTCCAACGCCGATCGGTCTCCCCC
S10 ATGCAATTCAAATACCTCATCGCTCTTTCTGCTCTCCTGCTCTCGAGCACGGTCATTGCGGCCCCCTTACCTGAGGGCACAACCAACGACGTCGTTCTCCAACGCCGATCGGTCTCCCCC
S11 ATGCAATTCAAATACCTCATCGCTCTTTCTGCTCTCCTGCTCTCGAGCACGGTCATTGCGGCCCCCTTACCTGAGGGCACAACCAACGACGTCGTTCTCCAACGCCGATCGGTCTCCCCC
S12 ATGCAATTCAAATACCTCATCGCTCTTTCTGCTCTCCTGCTCTCGAGCACGGTCATTGCGGCCCCCTTACCTGAGGGCACAACCAACGACGTCGTTCTCCAACGCCGATCGGTCTCCCCC
S13 ATGCAATTCAAATACCTCATCGCTCTTTCTGCTCTCCTGCTCTCGAGCACGGTCATTGCGGCCCCCTTACCTGAGGGCACAACCAACGACGTCGTTCTCCAACGCCGATCGGTCTCCCCC
S14 ATGCAATTCAAATACCTCATCGCTCTTTCTGCTCTCCTGCTCTCGAGCACGGTCATTGCGGCCCCCTTACCTGAGGGCACAACCAACGACGTCGTTCTCCAACGCCGATCGGTCTCCCCC
S15 ATGCAATTCAAATACCTCATCGCTCTTTCTGCTCTCCTGCTCTCGAGCACGGTCATTGCGGCCCCCTTACCTGAGGGCACAACCAACGACGTCGTTCTCCAACGCCGATCGGTCTCCCCC
180
240
S1 TCATACACGTTCACCAACGACTTGGCCGACATCGTGATCCCCGCCCCCCTCCCCGCGACCGCCGCTAAGAAAGCCATTGCCGCGCAGAACAAGAAGATCACAAAGGCAAAGGCGAACCAA
S2 TCATACACGTTCACCAACGACTTGGCCGACATCGTGATCCCCGCCCCCCTCCCCGCGACCGCTGCTAAGAAAGCCATCGCCGCGCAGAACAAGAAGATCACAAAGGCAAAGGCGAACCAA
S3 TCATACACGTTCACCAACGACTTGGCCGACATCGTGATCCCCGCCCCCCTCCCCGCGACCGCCGCTAAGAAAGCCATTGCCGCGCAGAACAAGAAGATCACAAAGGCAAAGGCGAACCAA
S4 TCATACACGTTCACCAACGACTTGGCCGACATCGTGATCCCCGCCCCCCTCCCCGCGACCGCTGCTAAGAAAGCCATCGCCGCGCAGAACAAGAAGATCACAAAGGCAAAGGCGAACCAA
S5 TCATACACGTTCACCAACGACTTGGCCGACATCGTGATCCCCGCCCCCCTCCCCGCGACCGCTGCTAAGAAAGCCATCGCCGCGCAGAACAAGAAGATCACAAAGGCAAAGGCGAACCAA
S6 TCATACACGTTCACCAACGACTTGGCCGACATCGTGATCCCCGCCCCCCTCCCCGCGACCGCTGCTAAGAAAGCCATCGCCGCGCAGAACAAGAAGATCACAAAGGCAAAGGCGAACCAA
S7 TCATACACGTTCACCAACGACTTGGCCGACATCGTGATCCCCGCCCCCCTCCCCGCGACCGCTGCTAAGAAAGCCATCGCCGCGCAGAACAAGAAGATCACAAAGGCAAAGGCGAACCAA
S8 TCATACACGTTCACCAACGACTTGGCCGACATCGTGATCCCCGCCCCCCTCCCCGCGACCGCTGCTAAGAAAGCCATCGCCGCGCAGAACAAGAAGATCACAAAGGCAAAGGCGAACCAA
S9 TCATACACGTTCACCAACGACTTGGCCGACATCGTGATCCCCGCCCCCCTCCCCGCGACCGCTGCTAAGAAAGCCATCGCCGCGCAGAACAAGAAGATCACAAAGGCAAAGGCGAACCAA
S10 TCATACACGTTCACCAACGACTTGGCCGACATCGTGATCCCCGCCCCCCTCCCCGCGACCGCTGCTAAGAAAGCCATCGCCGCGCAGAACAAGAAGATCACAAAGGCAAAGGCGAACCAA
S11 TCATACACGTTCACCAACGACTTGGCCGACATCGTGATCCCCGCCCCCCTCCCCGCGACCGCTGCTAAGAAAGCCATCGCCGCGCAGAACAAGAAGATCACAAAGGCAAAGGCGAACCAA
S12 TCATACACGTTCACCAACGACTTGGCCGACATCGTGATCCCCGCCCCCCTCCCCGCGACCGCTGCTAAGAAAGCCATCGCCGCGCAGAACAAGAAGATCACAAAGGCAAAGGCGAACCAA
S13 TCATACACGTTCACCAACGACTTGGCCGACATCGTGATCCCCGCCCCCCTCCCCGCGACCGCTGCTAAGAAAGCCATCGCCGCGCAGAACAAGAAGATCACAAAGGCAAAGGCGAACCAA
S14 TCATACACGTTCACCAACGACTTGGCCGACATCGTGATCCCCGCCCCCCTCCCCGCGACCGCTGCTAAGAAAGCCATCGCCGCGCAGAACAAGAAGATCACAAAGGCAAAGGCGAACCAA
S15 TCATACACGTTCACCAACGACTTGGCCGACATCGTGATCCCCGCCCCCCTCCCCGCGACCGCTGCTAAGAAAGCCATCGCCGCGCAGAACAAGAAGATCACAAAGGCAAAGGCGAACCAA
300
360
S1 AAGGCGAAGGAAGCCCTCCAGAAGACCGCGTCGTCGCACGTCACCACCGTCCTTAACGCGGCCGCTGGCACCCTGAACCTCAGCGGGAACCTTGCGGTCAAGGTCACAAACGACTTCCAC
S2 AAGGCGAAGGAAGCCCTCCAGAAGACCGCGTCGTCGCACGTCACCACCGTCCTTAACGCGGCCGCTGGCACCCTGAACCTCAGCGGGAACCTTGCGGTCAAGGTCACAAACGACTTCCAC
S3 AAGGCGAAGGAAGCCCTCCAGAAGACCGCGTCGTCGCACGTCACCACCGTCCTTAACGCGGCCGCTGGCACCCTGAACCTCAGCGGGAACCTTGCGGTCAAGGTCACAAACGACTTCCAC
S4 AAGGCGAAGGAAGCCCTCCAGAAGACCGCGTCGTCGCACGTCACCACCGTCCTTAACGCGGCCGCTGGCACCCTGAACCTCAGCGGGAACCTTGCGGTCAAGGTCACAAACGACTTCCAC
S5 AAGGCGAAGGAAGCCCTCCAGAAGACCGCGTCGTCGCACGTCACCACCGTCCTTAACGCGGCCGCTGGCACCCTGAACCTCAGCGGGAACCTTGCGGTCAAGGTCACAAACGACTTCCAC
S6 AAGGCGAAGGAAGCCCTCCAGAAGACCGCGTCGTCGCACGTCACCACCGTCCTTAACGCGGCCGCTGGCACCCTGAACCTCAGCGGGAACCTTGCGGTCAAGGTCACAAACGACTTCCAC
S7 AAGGCGAAGGAAGCCCTCCAGAAGACCGCGTCGTCGCACGTCACCACCGTCCTTAACGCGGCCGCTGGCACCCTGAACCTCAGCGGGAACCTTGCGGTCAAGGTCACAAACGACTTCCAC
S8 AAGGCGAAGGAAGCCCTCCAGAAGACCGCGTCGTCGCACGTCACCACCGTCCTTAACGCGGCCGCTGGCACCCTGAACCTCAGCGGGAACCTTGCGGTCAAGGTCACAAACGACTTCCAC
S9 AAGGCGAAGGAAGCCCTCCAGAAGACCGCGTCGTCGCACGTCACCACCGTCCTTAACGCGGCCGCTGGCACCCTGAACCTCAGCGGGAACCTTGCGGTCAAGGTCACAAACGACTTCCAC
S10 AAGGCGAAGGAAGCCCTCCAGAAGACCGCGTCGTCGCACGTCACCACCGTCCTTAACGCGGCCGCTGGCACCCTGAACCTCAGCGGGAACCTTGCGGTCAAGGTCACAAACGACTTCCAC
S11 AAGGCGAAGGAAGCCCTCCAGAAGACCGCGTCGTCGCACGTCACCACCGTCCTTAACGCGGCCGCTGGCACCCTGAACCTCAGCGGGAACCTTGCGGTCAAGGTCACAAACGACTTCCAC
S12 AAGGCGAAGGAAGCCCTCCAGAAGACCGCGTCGTCGCACGTCACCACCGTCCTTAACGCGGCCGCTGGCACCCTGAACCTCAGCGGGAACCTTGCGGTCAAGGTCACAAACGACTTCCAC
S13 AAGGCGAAGGAAGCCCTCCAGAAGACCGCGTCGTCGCACGTCACCACCGTCCTTAACGCGGCCGCTGGCACCCTGAACCTCAGCGGGAACCTTGCGGTCAAGGTCACAAACGACTTCCAC
S14 AAGGCGAAGGAAGCCCTCCAGAAGACCGCGTCGTCGCACGTCACCACCGTCCTTAACGCGGCCGCTGGCACCCTGAACCTCAGCGGGAACCTTGCGGTCAAGGTCACAAACGACTTCCAC
S15 AAGGCGAAGGAAGCCCTCCAGAAGACCGCGTCGTCGCACGTCACCACCGTCCTTAACGCGGCCGCTGGCACCCTGAACCTCAGCGGGAACCTTGCGGTCAAGGTCACAAACGACTTCCAC

```
                                                                              420                                                          480
S1    ACCAGCAAGGACCCGGAGAGCCACGCGACGTTCGAGTTCTCTGCGACTGCTTGTGGCGGGACGTGCGTCGGCCATGCGTACAAGTCGCCCTCGAAAATCTCGCCGGGCAAGGGCCAGCCC
S2    ACCAGCAAGGACCCGGAGAGCCACGCGACGTTCGAGTTCTCTGCGACTGCTTGTGGCGGGACGTGCGTCGGCCATGCGTACAAGTCGCCCTCGAAAATCTCGCCGGGCAAGGGCCAGCCC
S3    ACCAGCAAGGACCCGGAGAGCCACGCGACGTTCGAGTTCTCTGCGACTGCTTGTGGCGGGACGTGCGTCGGCCATGCGTACAAGTCGCCCTCGAAAATCTCGCCGGGCAAGGGCCAGCCC
S4    ACCAGCAAGGACCCGGAGAGCCACGCGACGTTCGAGTTCTCTGCGACTGCTTGTGGCGGGACGTGCGTCGGCCATGCGTACAAGTCGCCCTCGAAAATCTCGCCGGGCAAGGGCCAGCCC
S5    ACCAGCAAGGACCCGGAGAGCCACGCGACGTTCGAGTTCTCTGCGACTGCTTGTGGCGGGACGTGCGTCGGCCATGCGTACAAGTCGCCCTCGAAAATCTCGCCGGGCAAGGGCCAGCCC
S6    ACCAGCAAGGACCCGGAGAGCCACGCGACGTTCGAGTTCTCTGCGACTGCTTGTGGCGGGACGTGCGTCGGCCATGCGTACAAGTCGCCCTCGAAAATCTCGCCGGGCAAGGGCCAGCCC
S7    ACCAGCAAGGACCCGGAGAGCCACGCGACGTTCGAGTTCTCTGCGACTGCTTGTGGCGGGACGTGCGTCGGCCATGCGTACAAGTCGCCCTCGAAAATCTCGCCGGGCAAGGGCCAGCCC
S8    ACCAGCAAGGACCCGGAGAGCCACGCGACGTTCGAGTTCTCTGCGACTGCTTGTGGCGGGACGTGCGTCGGCCATGCGTACAAGTCGCCCTCGAAAATCTCGCCGGGCAAGGGCCAGCCC
S9    ACCAGCAAGGACCCGGAGAGCCACGCGACGTTCGAGTTCTCTGCGACTGCTTGTGGCGGGACGTGCGTCGGCCATGCGTACAAGTCGCCCTCGAAAATCTCGCCGGGCAAGGGCCAGCCC
S10   ACCAGCAAGGACCCGGAGAGCCACGCGACGTTCGAGTTCTCTGCGACTGCTTGTGGCGGGACGTGCGTCGGCCATGCGTACAAGTCGCCCTCGAAAATCTCGCCGGGCAAGGGCCAGCCC
S11   ACCAGCAAGGACCCGGAGAGCCACGCGACGTTCGAGTTCTCTGCGACTGCTTGTGGCGGGACGTGCGTCGGCCATGCGTACAAGTCGCCCTCGAAAATCTCGCCGGGCAAGGGCCAGCCC
S12   ACCAGCAAGGACCCGGAGAGCCACGCGACGTTCGAGTTCTCTGCGACTGCTTGTGGCGGGACGTGCGTCGGCCATGCGTACAAGTCGCCCTCGAAAATCTCGCCGGGCAAGGGCCAGCCC
S13   ACCAGCAAGGACCCGGAGAGCCACGCGACGTTCGAGTTCTCTGCGACTGCTTGTGGCGGGACGTGCGTCGGCCATGCGTACAAGTCGCCCTCGAAAATCTCGCCGGGCAAGGGCCAGCCC
S14   ACCAGCAAGGACCCGGAGAGCCACGCGACGTTCGAGTTCTCTGCGACTGCTTGTGGCGGGACGTGCGTCGGCCATGCGTACAAGTCGCCCTCGAAAATCTCGCCGGGCAAGGGCCAGCCC
S15   ACCAGCAAGGACCCGGAGAGCCACGCGACGTTCGAGTTCTCTGCGACTGCTTGTGGCGGGACGTGCGTCGGCCATGCGTACAAGTCGCCCTCGAAAATCTCGCCGGGCAAGGGCCAGCCC

                                                          534
S1    GGCAAAATCTTCAGCGCCGGGCATGCTGTTATTTTCGGGGGCAGCGATAAATGA
S2    GGCAAAATCTTCAGCGCCGGGCATGCTGTTATTTTCGGGGGCAGCGATAAATGA
S3    GGCAAAATCTTCAGCGCCGGGCATGCTGTTATTTTCGGGGGCAGCGATAAATGA
S4    GGCAAAATCTTCAGCGCCGGGCATGCTGTTATTTTCGGGGGCAGCGATAAATGA
S5    GGCAAAATCTTCAGCGCCGGGCATGCTGTTATTTTCGGGGGCAGCGATAAATGA
S6    GGCAAAATCTTCAGCGCCGGGCATGCTGTTATTTTCGGGGGCAGCGATAAATGA
S7    GGCAAAATCTTCAGCGCCGGGCATGCTGTTATTTTCGGGGGCAGCGATAAATGA
S8    GGCAAAATCTTCAGCGCCGGGCATGCTGTTATTTTCGGGGGCAGCGATAAATGA
S9    GGCAAAATCTTCAGCGCCGGGCATGCTGTTATTTTCGGGGGCAGCGATAAATGA
S10   GGCAAAATCTTCAGCGCCGGGCATGCTGTTATTTTCGGGGGCAGCGATAAATGA
S11   GGCAAAATCTTCAGCGCCGGGCATGCTGTTATTTTCGGGGGCAGCGATAAATGA
S12   GGCAAAATCTTCAGCGCCGGGCATGCTGTTATTTTCGGGGGCAGCGATAAATGA
S13   GGCAAAATCTTCAGCGCCGGGCATGCTGTTATTTTCGGGGGCAGCGATAAATGA
S14   GGCAAAATCTTCAGCGCCGGGCATGCTGTTATTTTCGGGGGCAGCGATAAATGA
S15   GGCAAAATCTTCAGCGCCGGGCATGCTGTTATTTTCGGGGGCAGCGATAAATGA
```

Table S1 Four HpSSP homologs in *H. parviporum* of HaSSPs

HpSSP	HaSSP	sequence discription	length (bp)	length(aa)	cysitine number
6,141	38	hypothetical protein	810	269	8
27,89	28	hypothetical protein	812	271	8
35,8	30	hypothetical protein	534	177	2
43,64	44	hypothetical protein	693	230	2

percent identity
94 %
86 %
93 %
90 %